A FLOW EQUATION APPROACH TO SEMI-CLASSICAL APPROXIMATIONS: A COMPARISON WITH THE WKB METHOD

By

Jacobus Daniël Thom

Thesis presented in partial fulfilment of the requirements for the degree of MASTER OF SCIENCE at the University of Stellenbosch.

Supervisor : Professor F G Scholtz

Co-supervisor : Professor H B Geyer

December 2006

DECLARATION

I, the undersigned, hereby declare that the work contained in this thesis is my own original work and that I have not previously in its entirety or in part submitted it at any university for a degree.

Signature

Date

ABSTRACT

The aim of this thesis is the semi-classical implementation of Wegner's flow equations and comparison with the well-established Wentzel-Kramers-Brillouin method. We do this by converting operators, in particular the Hamiltonian, into scalar functions, while an isomorphism with the operator product is maintained by the introduction of the Moyal product. A flow equation in terms of these scalar functions is set up and then approximated by expanding it to first order in $\hbar$. We apply this method to two potentials, namely the quartic anharmonic oscillator and the symmetric double-well potential. Results obtained via the flow equations are then compared with those obtained from the WKB method.

OPSOMMING

Die doel van hierdie tesis is die semi-klassieke implementering van Wegner se vloei-vergelykings en vergelyking met die welbekende Wentzel-Kramers-Brillouin metode. Ons doen dit deur operatore, en spesifiek die Hamilton operator, met skalare funksies te vervang, terwyl 'n isomorfisme met die operator produk behou word deur die invoering van die Moyal produk. 'n Vloei-vergelyking in terme van hierdie skalare funksies word opgestel en dan benader deur dit uit te brei tot eerste order in $\hbar$. Ons pas hierdie metode toe op twee potensiale, naamlik die kwarties nie-harmoniese ossillator en die simmetriese dubbelput potensiaal. Resultate wat ons verkry vanaf die vloei-vergelykings word dan vergelyk met dié verkry vanaf die WKB metode.

CONTENTS

LIST OF FIGURES

Introduction

Flow equations, in the form used in this work, were introduced fairly recently by Wegner [1] and separately by Glazek and Wilson [2]. This (exact) approach offers us a powerful new tool in the analysis of quantum systems. In this thesis, we combine the flow equations with the Moyal product [3], which enables a semi-classical approximation to the exact flow equations. We make this non-perturbative approximation, because perturbation theory fails in many interesting cases, such as the symmetric double-well potential (which we discuss in chapter 4). While other semi-classical approximations exist (e.g. the WKB method), it is often difficult to implement them or find higher order terms in their expansion. In the semi-classical formulation used in this thesis, the double commutators one has in the flow equation are replaced with so-called Moyal brackets. These Moyal brackets are very easy to expand to any order of $\hbar$ that one would like, therefore making the calculation of successive terms in the expansion a straight-forward task.

To verify the validity of our semi-classical approximation, we compare our results with those of one of the oldest and most well-established techniques, namely the Wentzel-Kramers-Brillouin or WKB method.

In the first chapter we provide a short overview of the WKB method. We start by looking at its basic assumption for validity, whereafter we move on to discuss aspects such as the classically allowed and forbidden regions and the connection formulas between the two. Finally we apply the WKB method to the symmetric double-well potential. Numerical results were generated for comparison with the Moyal bracket method's results of chapter 4.

The second chapter deals with the Moyal product and flow equation techniques we use throughout the rest of the work. The chapter ends by showing how to combine the two to form our semi-classical approximation.

Chapters three and four are applications of the Moyal bracket method to first the quartic anharmonic oscillator and then the more complicated symmetric double-well potential. In each chapter a comparison is given between the results obtained via the Moyal bracket method and the WKB approach. The results from the Moyal bracket approach are new and clearly show their worth in being able to obtain good results for the symmetric double-well

potential, a potential which cannot be treated perturbatively with any accuracy.

CHAPTER 1
The WKB Method

The Wentzel-Kramers-Brillouin method is one of the cornerstone methods of semi-classical approximation and any new approach should be tested against it. With this said, we will now give an overview of the WKB approximation [4, 5, 6].

1.1 Overview

In essence, the WKB method gives us approximate solutions to the Schrödinger equation. To see the idea behind this approximation, let us consider the following situation in one dimension: A particle with energy E is moving in a region where the potential $V(x)$ is constant. Then, if $E > V$, we can satisfy the Schrödinger equation with a wave function of the form

$$\psi(x) = Ae^{\pm ikx}, \quad \text{with} \quad k \equiv \frac{1}{\hbar}\sqrt{2m(E-V)}. \tag{1.1}$$

This is a plane wave traveling in the direction indicated by the plus (to the right) or the minus (to the left). It also has a constant wavelength $\lambda = \frac{2\pi}{k}$ and a constant amplitude A. This ideal case of a constant potential is, however, not very realistic in general. On the other hand, one might not be able to solve for an arbitrary potential $V(x)$. This is were the WKB approximation comes in: If $V(x)$ is not constant, but varies very slowly in comparison to λ, then we may say that the potential is still essentially constant and the wave function will still be sinusoidal for all intents and purposes. The wavelength and amplitude, however, now become slowly varying functions of x.

In the case where $E < V$ (V constant) a similar argument may be followed, except that the wave function ψ is now exponential:

$$\psi(x) = Ae^{\pm\kappa x}, \quad \text{with} \quad \kappa \equiv \frac{1}{\hbar}\sqrt{2m(V-E)}. \tag{1.2}$$

Then if $V(x)$ is not constant, but once again changes slowly in comparison to $\frac{1}{\kappa}$, ψ remains in essence exponential, where A and κ now change slowly with x.

There is one thing we have not yet touched upon, namely when $E \approx V$. In the region of these classical turning points we find that both $\frac{1}{k}$ (and hence the wavelength) and $\frac{1}{\kappa}$ tend

to infinity. We can therefore not assert that $V(x)$ changes slowly by comparison to the length scale on which the wave function varies, in this region. In the actual application of the WKB method, great care should then be taken to correctly handle these points.

1.1.1 The $E > V(x)$ region

Let us now turn to the so-called classical region, where $E > V(x)$, and find a mathematical expression for our approximate wave function in the WKB framework. First let us rewrite the Schrödinger equation in a different form:

$$\begin{aligned} -\frac{\hbar^2}{2m}\frac{d^2\psi}{dx^2} &+ V(x)\psi(x) = E\psi(x) \\ \frac{d^2\psi}{dx^2} &= -\frac{p(x)^2}{\hbar^2}\psi(x), \end{aligned} \tag{1.3}$$

where $p(x) = \sqrt{2m(E - V(x))}$ is of course the classical momentum for a particle with energy E and potential energy $V(x)$.

We can, in general, write the wave function of a particle in a form using an amplitude and a phase:

$$\psi(x) = A(x)e^{i\phi(x)}, \tag{1.4}$$

where both $A(x)$ and $\phi(x)$ are real functions. Let us now substitute this into the second form of the Schrödinger equation, (1.3):

$$\begin{aligned} \frac{d\psi}{dx} &= (A'(x) + iA(x)\phi'(x))e^{i\phi(x)} \\ \frac{d^2\psi}{dx^2} &= (A'' + 2iA'\phi' + iA\phi'' - A(\phi')^2)e^{i\phi} \\ A'' &+ 2iA'\phi' + iA\phi'' - A(\phi')^2 = -\frac{p^2}{\hbar^2}A. \end{aligned} \tag{1.5}$$

Here we have used primes to indicate derivatives to x. Equation (1.5) is actually two equations in disguise. One for the real part and one for the imaginary part. Separating them gives us

$$A'' - A(\phi')^2 = -A\frac{p^2}{\hbar^2} \tag{1.6}$$

$$2A'\phi' + A\phi'' = 0. \tag{1.7}$$

We can write both of these equations in forms which make it clearer how to solve them:

$$A'' = A\left((\phi')^2 - \frac{p^2}{\hbar^2}\right) \tag{1.8}$$

$$(A^2\phi')' = 0. \tag{1.9}$$

$A(x)$ is not the zero function, since we are not interested in trivial solutions of the Schrödinger equation. The second equation (eq. 1.9) can now be easily solved:

$$A^2\phi' = C^2 \quad \text{or alternatively} \quad A = \frac{C}{\sqrt{\phi'}}. \tag{1.10}$$

Here we take only the positive solution, since $A(x)$ is an amplitude. The first equation (eq. 1.8), however, cannot be solved in general. Here, therefore, is where the approximation, upon which the WKB method rests, comes in: We will assume that the amplitude, A, varies very slowly, so that the ratio $\frac{A''}{A}$ becomes negligible in comparison to both $(\phi')^2$ and $\frac{p^2}{\hbar^2}$. This reduces the left hand side of (1.8) to zero, so that we obtain:

$$(\phi')^2 = \frac{p^2}{\hbar^2} \quad \Rightarrow \quad \phi' = \pm\frac{p}{\hbar}. \tag{1.11}$$

We can then integrate to find for $\phi(x)$

$$\phi(x) = \pm\frac{1}{\hbar}\int p(x)dx, \tag{1.12}$$

which then gives us

$$\psi(x) = \frac{C}{\sqrt{p(x)}}e^{\pm\frac{i}{\hbar}\int p(x)dx}. \tag{1.13}$$

The general form of $\psi(x)$ is of course a linear combination of the terms with different signs:

$$\psi(x) = \frac{1}{\sqrt{p(x)}}\left(\alpha e^{\frac{i}{\hbar}\int p(x)dx} + \beta e^{-\frac{i}{\hbar}\int p(x)dx}\right), \tag{1.14}$$

where we have absorbed the constant C into both α and β.

1.1.2 The $E < V(x)$ region

While we have taken $E > V(x)$ in the above discussion, it can easily be seen that when $E < V(x)$, such as when a particle enters a potential barrier, we find that $p(x)$ becomes imaginary. This simply turns $p(x)$ into $i|p(x)|$ so that we obtain for the wave function,

$$\psi(x) = \frac{C}{\sqrt{|p(x)|}} e^{\pm \frac{1}{\hbar} \int |p(x)| dx}. \tag{1.15}$$

The general solution is of course once again a linear combination of the two terms, one with a plus sign and one with a minus sign. However, in this case the coefficient of the exponentially growing term must be small, and indeed zero for a barrier of infinite width, in order to ensure quadratic integrability of the wave function.

1.1.3 Connection Formulas

We now have formulas for the wave function in the case where the particle's total energy is greater than the potential, as well as for the case where the particle's energy is less. We will now turn our discussion to the region where the WKB method breaks down and how to deal with this problem.

The WKB method starts to fail once we are close enough to a classical turning point, i.e. when $E \approx V(x)$, since then $p(x) \to 0$ and the wave function goes to infinity. What we need, therefore, is some kind of wave function that works in this area and that can bridge the small gap between the wave functions on either side (above and below) of the potential. For the sake of the following discussion, we assume that the point where $E = V(x)$ occurs at $x = a$. Close to this point we can approximate $V(x)$ by a straight line,

$$V(x) \cong V(a) + V'(a)(x - a) = E + V'(a)(x - a). \tag{1.16}$$

We now need to find the wave function for this linearised potential, so we need to solve the Schrödinger equation,

$$-\frac{\hbar^2}{2m} \frac{d^2\xi}{dx^2} + (E + V'(a)(x - a))\xi = E\xi. \tag{1.17}$$

This can be written as

$$\frac{d^2\xi}{dx^2} = \kappa^3(x-a)\xi, \quad \text{where} \quad \kappa = \left(\frac{2mV'(a)}{\hbar^2}\right)^{\frac{1}{3}}. \tag{1.18}$$

By additionally setting $z = \kappa(x-a)$, we obtain Airy's equation,

$$\frac{d^2\xi}{dz^2} = z\xi, \tag{1.19}$$

with solutions $Ai(z)$ and $Bi(z)$ (since the Airy equation is a second order linear differential equation). Once again the general solution for ξ is a linear combination of $Ai(z)$ and $Bi(z)$:

$$\xi(x) = c\,Ai(\kappa(x-a)) + d\,Bi(\kappa(x-a)), \tag{1.20}$$

with c and d appropriately chosen. We have assumed here that $V'(a)$ is positive (upward-sloping turning point), so that κ is real. However, if $V'(a)$ is negative (downward-sloping turning point) we can simply define $\kappa = -\left(\frac{2m|V'(a)|}{\hbar^2}\right)^{\frac{1}{3}}$ without altering the above discussion.

The following is a list of the asymptotic forms of the two Airy functions. We shall be using them in order to connect the wave functions together.

For $z \gg 0$:

$$Ai(z) \sim \frac{1}{2\sqrt{\pi}z^{1/4}}e^{-\frac{2}{3}z^{3/2}} \tag{1.21}$$

$$Bi(z) \sim \frac{1}{\sqrt{\pi}z^{1/4}}e^{\frac{2}{3}z^{3/2}}. \tag{1.22}$$

For $z \ll 0$:

$$Ai(z) \sim \frac{1}{\sqrt{\pi}(-z)^{1/4}}\sin\left[\frac{2}{3}(-z)^{\frac{3}{2}} + \frac{\pi}{4}\right] \tag{1.23}$$

$$Bi(z) \sim \frac{1}{\sqrt{\pi}(-z)^{1/4}}\cos\left[\frac{2}{3}(-z)^{\frac{3}{2}} + \frac{\pi}{4}\right]. \tag{1.24}$$

We now need to match the WKB solutions on either side of $x = a$ to the wave function $\xi(x)$. This needs to be done in a region where the following conditions hold: The linearised potential $E + V'(a)(x-a)$ needs to remain accurate enough such that $\xi(x)$ remains a good

approximation and it needs to extend far enough from $x = a$ so that the WKB wave functions remain reliable.

For the derivation of the connection formulas we will confine our discussion to a upwards-sloping turning point as the derivation for a downward-sloping turning point is very similar. From our discussion of the WKB solutions in sections 1.1.1 and 1.1.2 we obtain as our WKB wave functions:

$$\psi_{WKB}(x) = \begin{cases} \frac{1}{\sqrt{p(x)}}\left[\alpha\, e^{\frac{i}{\hbar}\int_x^a p(x')dx'} + \beta\, e^{-\frac{i}{\hbar}\int_x^a p(x')dx'}\right], & x < a \\ \frac{1}{\sqrt{|p(x)|}}\left[\gamma\, e^{\frac{1}{\hbar}\int_a^x |p(x')|dx'} + \delta\, e^{-\frac{1}{\hbar}\int_a^x |p(x')|dx'}\right], & x > a \end{cases} \tag{1.25}$$

If we take $E < V(x)$ for all $x > a$, then we must take $\gamma = 0$. Futhermore, in this overlapping region we may use the approximate potential (1.16) to calculate $\psi_{WKB}(x)$:

$$p(x) \approx \sqrt{2m[E - E - V'(a)(x-a)]} = \sqrt{-2mV'(a)(x-a)} = \hbar\,\kappa^{\frac{3}{2}}\sqrt{-(x-a)}. \tag{1.26}$$

Therefore in the $x > a$ region we find,

$$\int_a^x |p(x')|dx' \approx \hbar\,\kappa^{\frac{3}{2}}\int_a^x \sqrt{-(x'-a)}dx' = \frac{2}{3}\hbar\kappa^{\frac{3}{2}}(x-a)^{\frac{3}{2}}, \tag{1.27}$$

so that

$$\psi_{WKB}(x) \approx \frac{\delta}{\sqrt{\hbar}\kappa^{3/4}(x-a)^{1/4}} e^{-\frac{2}{3}[\kappa(x-a)]^{3/2}}. \tag{1.28}$$

Now, using the asymptotic form of the Airy functions ($x \gg a \Rightarrow z \gg 0$), we obtain for ξ:

$$\xi(x) \approx \frac{c}{2\sqrt{\pi}[\kappa(x-a)]^{1/4}} e^{-\frac{2}{3}[\kappa(x-a)]^{3/2}} + \frac{d}{\sqrt{\pi}[\kappa(x-a)]^{1/4}} e^{\frac{2}{3}[\kappa(x-a)]^{3/2}}. \tag{1.29}$$

Comparing (1.28) and (1.29) we see that

$$c = 2\sqrt{\frac{\pi}{\hbar\kappa}}\delta \tag{1.30}$$

$$d = 0. \tag{1.31}$$

We can now repeat this procedure for the region where $x < a$:

$$\int_x^a p(x')dx' \approx \hbar\,\kappa^{\frac{3}{2}} \approx \int_x^a \sqrt{-(x'-a)}dx' = \frac{2}{3}\hbar[-\kappa(x-a)]^{\frac{3}{2}}. \tag{1.32}$$

$$\psi_{WKB}(x) \approx \frac{1}{\sqrt{\hbar}\kappa^{3/4}(-(x-a))^{1/4}}\left[\alpha\, e^{i\frac{2}{3}[-\kappa(x-a)]^{\frac{3}{2}}} + \beta\, e^{-i\frac{2}{3}[-\kappa(x-a)]^{\frac{3}{2}}}\right] \tag{1.33}$$

Once again we use the Airy functions' asymptotic form ($x \ll a \Rightarrow z \ll 0$) to write for $\xi(x)$,

$$\begin{aligned}\xi(x) &\approx \frac{c}{\sqrt{\pi}[-\kappa(x-a)]^{1/4}}\sin\left[\frac{2}{3}[-\kappa(x-a)]^{2/3} + \frac{\pi}{4}\right] \\ &= \frac{1}{2i}\frac{c}{\sqrt{\pi}[-\kappa(x-a)]^{1/4}}\left[e^{i\pi/4}e^{i\frac{2}{3}[-\kappa(x-a)]^{2/3}} - e^{-i\pi/4}e^{-i\frac{2}{3}[-\kappa(x-a)]^{2/3}}\right],\end{aligned} \tag{1.34}$$

(remember $d = 0$).

Comparing (1.33) and (1.34) this time and using (1.30) gives us

$$\frac{c}{2i\sqrt{\pi}}e^{i\pi/4} = \frac{2\sqrt{\frac{\pi}{\hbar\kappa}}\delta}{2i\sqrt{\pi}}e^{i\pi/4} = \frac{\delta}{i\sqrt{\hbar\kappa}}e^{i\pi/4} = \frac{\alpha}{\sqrt{\hbar\kappa}} \quad \Rightarrow \quad \alpha = -ie^{i\pi/4}\delta \tag{1.35}$$

$$\frac{-c}{2i\sqrt{\pi}}e^{-i\pi/4} = \frac{-2\sqrt{\frac{\pi}{\hbar\kappa}}\,\delta}{2i\sqrt{\pi}}e^{-i\pi/4} = \frac{-\delta}{i\sqrt{\hbar\kappa}}e^{-i\pi/4} = \frac{\beta}{\sqrt{\hbar\kappa}} \quad \Rightarrow \quad \beta = ie^{-i\pi/4}\delta. \tag{1.36}$$

The above are the so-called connection formulas which allow a smooth transition from one side of the turning point to the other. We can now express the WKB wave function in terms of a single normalization constant δ:

$$\psi_{WKB}(x) = \begin{cases} \frac{2\delta}{\sqrt{p(x)}}\sin\left[\frac{1}{\hbar}\int_x^a p(x')dx' + \frac{\pi}{4}\right], & x < a \\ \frac{\delta}{\sqrt{|p(x)|}}\left[e^{-\frac{1}{\hbar}\int_a^x |p(x')|dx'}\right], & x > a \end{cases} \tag{1.37}$$

1.2 Example: The Symmetric Double-Well Potential

In this section we will apply the WKB method to a symmetric double-well potential. We will use the results obtained this way as a comparison to our findings in a later chapter.

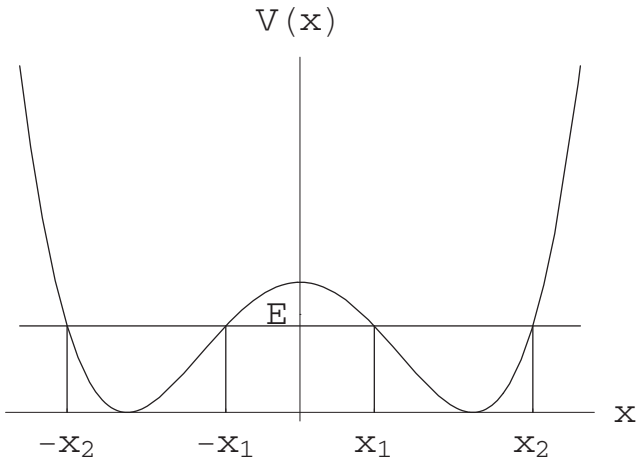

Figure 1.1: The general form of the symmetric double-well potential

1.2.1 The WKB wave function

The form of the potential we shall be looking at is the following (see Figure 1.1)

$$V(x) = -ax^2 + bx^4 + \frac{a^2}{4b} \tag{1.38}$$

$$= \frac{(a - 2bx^2)^2}{4b}, \tag{1.39}$$

where $a, b > 0$.

Since this potential is symmetric we need only concern ourselves with even and odd wave functions. In particular, we will obtain the wave functions for when $E < V(0)$. First we write down the general forms of the WKB wave functions in the regions $0 < x < x_1$, $x_1 < x < x_2$ and $x > x_2$:

$$\psi_{WKB}(x) = \begin{cases} \frac{1}{\sqrt{|p(x)|}} \left[\delta\, e^{-\frac{1}{\hbar}\int_{x_2}^{x} |p(x')|dx'} \right], & x > x_2 \\ \frac{1}{\sqrt{p(x)}} \left[\alpha\, e^{\frac{i}{\hbar}\int_{x}^{x_2} p(x')dx'} + \beta\, e^{-\frac{i}{\hbar}\int_{x}^{x_2} p(x')dx'} \right], & x_1 < x < x_2 \\ \frac{1}{\sqrt{|p(x)|}} \left[\eta\, e^{\frac{1}{\hbar}\int_{x}^{x_1} |p(x')|dx'} + \rho\, e^{-\frac{1}{\hbar}\int_{x}^{x_1} |p(x')|dx'} \right], & 0 < x < x_1. \end{cases} \tag{1.40}$$

We cannot assume that η is zero, since our barrier is not infinitely wide. We have already done most of the work for the turning point x_2 in section 1.1.3, so we will simply write:

$$\psi_{WKB}(x) = \begin{cases} \frac{1}{\sqrt{|p(x)|}}\left[\delta\, e^{-\frac{1}{\hbar}\int_{x_2}^{x}|p(x')|dx'}\right], & x > x_2 \\ \frac{2\delta}{\sqrt{p(x)}}\sin\left[\frac{1}{\hbar}\int_{x}^{x_2}p(x')dx' + \frac{\pi}{4}\right], & x_1 < x < x_2 \end{cases} \tag{1.41}$$

Now we need to obtain the connection formulas for the wave functions at x_1. Analysis proceeds just as in section 1.1.3. There are, of course, some small changes to be made. With $a = x_1$, $\kappa = \left[\frac{2m}{\hbar^2}|V'(x_1)|\right]^{1/3}$ and $z = -\kappa(x - x_1)$ we can once again use the Airy functions just as before to write the bridging wave function as

$$\xi(x) = c\,Ai(-\kappa(x - x_1)) + d\,Bi(-\kappa(x - x_1)). \tag{1.42}$$

Once again we have that

$$p(x) \approx \sqrt{2m[E - E - V'(x_1)(x - x_1)]} = \sqrt{-2mV'(x_1)(x - x_1)}, \tag{1.43}$$

however, since $V'(x_1)$ is negative, we have that $-V'(x_1) = |V'(x_1)|$ so that

$$p(x) \approx \hbar\,\kappa^{\frac{3}{2}}\sqrt{(x - x_1)}. \tag{1.44}$$

Left of the turning point x_1 (i.e. region $0 < x < x_1$) this leads to

$$\int_x^{x_1}|p(x')|dx' = \hbar\kappa^{3/2}\int_x^{x_1}(x_1 - x')^{1/2}dx' \tag{1.45}$$

$$= \frac{2}{3}\hbar\kappa^{3/2}\left[-(x_1 - x')^{3/2}\right]_x^{x_1} \tag{1.46}$$

$$= \frac{2}{3}\hbar(-\kappa(x - x_1))^{3/2}. \tag{1.47}$$

We can then write $\psi_{WKB}(x)$ approximately as

$$\psi_{WKB}(x) \approx \frac{1}{\sqrt{\hbar}\kappa^{3/4}(x_1 - x)^{1/4}}\left[\eta\, e^{\frac{2}{3}(-\kappa(x-x_1))^{3/2}} + \rho\, e^{-\frac{2}{3}(-\kappa(x-x_1)}\right]. \tag{1.48}$$

If $x - x_1 \ll 0 \Rightarrow z \gg 0$, so that, using the asymptotic forms of the Airy functions, we

have for the bridging wave function ξ:

$$\xi(x) \approx \frac{c}{2\sqrt{\pi}(\kappa(x_1-x))^{1/4}} e^{-\frac{2}{3}(-\kappa(x-x_1)^{3/2}} + \frac{d}{\sqrt{\pi}(\kappa(x_1-x))^{1/4}} e^{\frac{2}{3}(-\kappa(x-x_1))^{3/2}}. \quad (1.49)$$

Comparing (1.48) and (1.49) we solve for c and d as such

$$c = \frac{2\sqrt{\pi}}{\sqrt{\hbar\kappa}}\rho \quad \text{and} \quad d = \frac{\sqrt{\pi}}{\sqrt{\hbar\kappa}}\eta. \quad (1.50)$$

Next, for the region $x_1 < x < x_2$ we integrate $p(x)$ and find

$$\int_{x_1}^{x} p(x')dx' \;=\; \frac{2}{3}\hbar(\kappa(x-x_1))^{3/2}. \quad (1.51)$$

The WKB approximation becomes

$$\psi_{WKB}(x) \approx \frac{1}{\sqrt{\hbar}\kappa^{3/4}(x-x_1)^{1/4}}\left[\alpha\, e^{\frac{2}{3}(\kappa(x-x_1))^{3/2}} + \beta\, e^{-\frac{2}{3}(\kappa(x-x_1)}\right] \quad (1.52)$$

and the bridging function ξ (using the $z \ll 0$ asymptotic forms of the Airy functions) becomes

$$\begin{aligned}\xi(x) \;&\approx\; \frac{c}{\sqrt{\pi}(\kappa(x-x_1))^{1/4}}\sin\left[\frac{2}{3}(\kappa(x-x_1))^{3/2}+\frac{\pi}{4}\right] \\ &\quad + \frac{d}{\sqrt{\pi}(\kappa(x-x_1))^{1/4}}\cos\left[\frac{2}{3}(\kappa(x-x_1))^{3/2}+\frac{\pi}{4}\right] \quad (1.53)\\ &= \frac{1}{\sqrt{\pi}(\kappa(x-x_1))^{1/4}}\left[\left(\frac{d}{2}+\frac{c}{2i}\right)e^{i\frac{\pi}{4}}e^{i\chi} + \left(\frac{d}{2}-\frac{c}{2i}\right)e^{-i\frac{\pi}{4}}e^{-i\chi}\right], \quad (1.54)\end{aligned}$$

where $\chi = \frac{2}{3}(\kappa(x-x_1))^{3/2}$, so that comparing (1.52) and (1.54) we can solve for α and β:

$$\alpha = \left(\frac{1}{2}\eta - i\rho\right)e^{i\frac{\pi}{4}} \quad \text{and} \quad \beta = \left(\frac{1}{2}\eta + i\rho\right)e^{-i\frac{\pi}{4}}. \quad (1.55)$$

Therefore

$$\psi_{WKB}(x) \approx \frac{1}{\sqrt{p(x)}}\left[\left(\frac{1}{2}\eta - i\rho\right)e^{i\frac{\pi}{4}}e^{\frac{i}{\hbar}\int_{x_1}^{x}p(x')dx'} + \left(\frac{1}{2}\eta + i\rho\right)e^{-i\frac{\pi}{4}}e^{-\frac{i}{\hbar}\int_{x_1}^{x}p(x')dx'}\right]. \quad (1.56)$$

Now we have two forms for the wave function in the region $x_1 < x < x_2$: one just derived and one from the connection formulas at x_2. We will now write the second line of

(1.41) in a more suggestive form to ease comparison:

$$\psi_{WKB}(x) = \frac{-i\delta}{\sqrt{p(x)}}\left[e^{i\frac{\pi}{4}}e^{\frac{i}{\hbar}\int_x^{x_2}p(x')dx'} - e^{-i\frac{\pi}{4}}e^{-\frac{i}{\hbar}\int_x^{x_2}p(x')dx'}\right] \tag{1.57}$$

$$= \frac{-i\delta}{\sqrt{p(x)}}\left[e^{i\frac{\pi}{4}}e^{\frac{i}{\hbar}\int_{x_1}^{x_2}p(x')dx'}e^{-\frac{i}{\hbar}\int_{x_1}^{x}p(x')dx'}\right.$$
$$\left.-e^{-i\frac{\pi}{4}}e^{-\frac{i}{\hbar}\int_{x_1}^{x_2}p(x')dx'}e^{\frac{i}{\hbar}\int_{x_1}^{x}p(x')dx'}\right]. \tag{1.58}$$

We can now easily compare (1.56) and (1.58) to obtain the following expressions:

$$i\delta\, e^{-i\frac{\pi}{2}}e^{-i\theta} = \frac{1}{2}\eta - i\rho \tag{1.59}$$

$$-i\delta\, e^{i\frac{\pi}{2}}e^{i\theta} = \frac{1}{2}\eta + i\rho, \tag{1.60}$$

where

$$\theta \equiv \frac{1}{\hbar}\int_{x_1}^{x_2}p(x')dx'. \tag{1.61}$$

Adding (1.59) and (1.60) we find

$$\eta = \frac{2\delta}{2i}\left(e^{i\theta+\frac{\pi}{2}} - e^{-\left(i\theta+\frac{\pi}{2}\right)}\right) = 2\delta\cos\theta. \tag{1.62}$$

Subtracting (1.59) from (1.60) we find in a similar fashion that

$$\rho = \delta\sin\theta. \tag{1.63}$$

After putting everything together we can write $\psi_{WKB}(x)$ in terms of a single normalization constant δ:

$$\psi_{WKB}(x) = \begin{cases} \frac{\delta}{\sqrt{|p(x)|}}\, e^{-\frac{1}{\hbar}\int_{x_2}^{x}|p(x')|dx'}, & x > x_2 \\ \frac{2\delta}{\sqrt{p(x)}}\sin\left[\frac{1}{\hbar}\int_x^{x_2}p(x')dx' + \frac{\pi}{4}\right], & x_1 < x < x_2 \\ \frac{\delta}{\sqrt{|p(x)|}}\left[2\cos(\theta)\, e^{\frac{1}{\hbar}\int_x^{x_1}|p(x')|dx'} + \sin(\theta)\, e^{-\frac{1}{\hbar}\int_x^{x_1}|p(x')|dx'}\right], & 0 < x < x_1 \end{cases} \tag{1.64}$$

1.2.2 Eigenvalues

We now use the fact that the wave functions are either even or odd. In the former case we must have that $\psi'(0) = 0$ and in the latter, $\psi(0) = 0$. In terms of the WKB wave function, this means that for the odd case

$$0 = \psi_{WKB}(0) = \frac{\delta}{\sqrt{|p(0)|}}\left[2\cos\theta\, e^{\frac{1}{\hbar}\int_0^{x_1}|p(x')|dx'} + \sin\theta\, e^{-\frac{1}{\hbar}\int_0^{x_1}|p(x')|dx'}\right] \tag{1.65}$$

$$\Rightarrow \tan\theta = -2e^{\frac{2}{\hbar}\int_0^{x_1}|p(x')|dx'} = -2e^{\frac{1}{\hbar}\int_{-x_1}^{x_1}|p(x')|dx'} = -2e^{\phi} \tag{1.66}$$

$$\phi \equiv \frac{1}{\hbar}\int_{-x_1}^{x_1}|p(x')|dx', \tag{1.67}$$

where we have made use of the symmetry of $|p(x)|$ around zero in the second step of the second equation and have assumed that $E < V(0)$.

Similarly for the even case

$$0 = \psi'_{WKB}(0) = \frac{\delta}{\sqrt{|p(0)|}}\left[2\cos\theta\,\frac{-1}{\hbar}|p(0)|e^{\frac{1}{\hbar}\int_0^{x_1}|p(x')|dx'} + \sin\theta\,\frac{1}{\hbar}|p(0)|e^{-\frac{1}{\hbar}\int_0^{x_1}|p(x')|dx'}\right] \tag{1.68}$$

$$\Rightarrow \tan\theta = 2e^{\frac{2}{\hbar}\int_0^{x_1}|p(x')|dx'} = 2e^{\phi}, \tag{1.69}$$

where we have use the facts that $\left.\frac{d|p(x)|}{dx}\right|_0 = 0$ and $\frac{d}{dx}\int_x^{x_1}|p(x')|dx' = -|p(x)|$.
Equations (1.66) and (1.69) give us the allowed energies, since both θ and ϕ are functions of energy E (x_1 and x_2 also depend on E).

In order to solve either (1.66) or (1.69) we will have to evaluate the integrals θ and ϕ. This is done most easily by numerical means since both θ and ϕ have elliptic integrals in their solution [7]. We can then (also numerically) find the values of E for which either (1.66) or (1.69) hold. These values are then the approximate energy eigenvalues of our Hamiltonian as given by the WKB method.

Table 1.1 gives us the first 10 eigenvalues as obtained in the WKB approximation. The 'exact' eigenvalues were obtained (numerically) by directly diagonalizing the matrix of the Hamiltonian, where we have truncated the matrix at a thousand by a thousand. The size of the matrix was then increased till the last significant digit of the eigenvalues (accross the region we are interested in) no longer changed. As one can see from the errors provided, the WKB approximation does very well. Accuracy also increases as the energy increases,

	Exact	WKB	Absolute Error	Relative Error
E_0	3.0553629439623435	3.062225635921198	0.0068626920	0.0022461135
E_1	3.055362943962443	3.062225635921198	0.0068626920	0.0022461135
E_2	9.054511016723644	9.062042116729279	0.0075311000	0.0008317512
E_3	9.054511016723914	9.062042116729753	0.0075311000	0.0008317512
E_4	14.875217917755847	14.88361048127084	0.0083925635	0.0005641977
E_5	14.875217917849273	14.883610481363226	0.0083925635	0.0005641976
E_6	20.499573023765766	20.509125531696096	0.0095525079	0.0004659857
E_7	20.499573034635606	20.509125542498584	0.0095525079	0.0004659857
E_8	25.904042009809086	25.915255556389386	0.0112135466	0.0004328879
E_9	25.904042852808853	25.91525639741849	0.0112135446	0.0004328878

Table 1.1: First ten energy eigenvalues of the symmetric double well potential (a = 9.5, b = 0.5)

	Exact	WKB	Absolute Error	Relative Error
E_{14}	40.34023869794828	40.371377784456584	0.0311390865	0.0007719113
E_{15}	40.382244854701284	40.41429520571597	0.0320503510	0.0007936743
E_{16}	43.95668645193638	44.021305354829 28	0.0646189029	0.0014700586
E_{17}	44.47492694456559	44.6081815391117	0.1332545945	0.0029961734

Table 1.2: Energy eigenvalues near hump of symmetric double well potential (a = 9.5, b = 0.5)

as one would expect from a semi-classical approximation, and as is explained in more detail below. However, this increase in accuracy does not continue throughout the spectrum. When one nears the top of the hump in the centre of the potential the approximation starts to do worse (Table 1.2). Once the hump is cleared accuracy improves once again.

The reason for the general trend in the WKB method that one does better for higher energies, stems, of course, from our assumptions about when it is valid in the first place. In section 1.1 we said that the WKB method may be applied if the potential varies sufficiently slowly in comparison to the wave length of the wave function. In other words, we want $\frac{\lambda}{l}$ to be small, where λ is the wave length and l is the length on which the potential varies significantly. At higher energies the wave length decreases. This improves $\frac{\lambda}{l}$ and thereby also our approximation. Furthermore, as $\lambda \to 0$ for higher energies, we can get closer to the turning point before the WKB wave function breaks down as an approximation. This means we need to linearise over smaller intervals, which increases accuracy even more. Additionally, our linearisation of the potential also becomes a better approximation for

$x_0 = 5$		$x_0 = 100$	
x	$\frac{\lvert V(x)-(V(x_0)+V'(x_0)(x-x_0))\rvert}{V(x)}$	x	$\frac{\lvert V(x)-(V(x_0)+V'(x_0)(x-x_0))\rvert}{V(x)}$
4	1	99	0.0006209878749853483
4.8	0.016720665090142334	99.8	0.000024180962419714326
4.85	0.008986181751460822	99.85	0.000013579081396532828
4.9	0.003818970662745555	99.9	$6.025076706858759 \times 10^{-6}$
4.95	0.0009136546034606218	99.95	$1.5037571998365037 \times 10^{-6}$
5	0	100	0
5.05	0.0008385967604778388	100.05	$1.498750187834707 \times 10^{-6}$
5.1	0.003217116755670 9875	100.1	$5.985020484314078 \times 10^{-6}$
5.15	0.006947066406272719	100.15	0.000013443890934778242
5.2	0.011860962249794903	100.2	0.000023860508596030646
6	0.16753381893860564	101	0.0005809149689237281

Table 1.3: Relative errors of linearisation of $V(x)$ (a = 10, b = 1)

steeper gradients. Consider, for example, equation (1.38) with $a = 10$ and $b = 1$. If one compares the relative error one makes by linearisation at $x = 5$ with $x = 100$ one obtains Table 1.3. It is clear that we make less of an error by linearising the potential the higher up in energy we go for $V(x)$. This is a general observation for the parts of potentials that have steeper gradients. The extreme case is of course the square well potential, where we need not linearise at all.

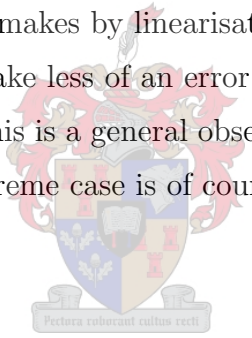

1.2.3 Level splitting

If one thinks of the symmetric double well potential classically, one realizes that if a particle in the potential has less energy than the top of the hump, it cannot leave the well and spends its time in either the left or the right well, depending on where it started. We therefore have in effect two completely separate wells, with degenerate energy eigenvalues (since the form of both wells is the same). Quantum mechanics teaches us, however, that the particle may tunnel through the barrier with an exponentially decaying probability. This tunneling lifts the denegeracy and creates two states with energies very close to each other. Once again, the WKB method provides us with a fairly good approximation to this splitting, at least for higher energies.

As one can see from Table 1.4 the WKB approximation, as we have implemented it, does not succeed in giving us the splitting in the ground state energy. However, it rapidly improves as the energy increases and starts to fail once more when the energy reaches a

	Exact	WKB	Relative Error
$E_1 - E_0$	$9.9475983006414 \times 10^{-14}$	0	1
$E_3 - E_2$	$2.70006239588838 \times 10^{-13}$	$4.7073456244106 \times 10^{-13}$	0.7434210526
$E_5 - E_4$	$9.3425711611416 \times 10^{-11}$	$9.2388319217207 \times 10^{-11}$	0.0111039282
$E_7 - E_6$	$1.08698401390938 \times 10^{-8}$	$1.08024877931711 \times 10^{-8}$	0.0061962591
$E_9 - E_8$	$8.4299976776947 \times 10^{-7}$	$8.4102910236083 \times 10^{-7}$	0.0023376820
$E_{11} - E_{10}$	0.000045397951858205	0.0000454631468720378	0.0014360783
$E_{13} - E_{12}$	0.00170014617764024	0.0017117430785518195	0.0068211199
$E_{15} - E_{14}$	0.04200615675300412	0.04291742125938924	0.0216935939
$E_{17} - E_{16}$	0.5182404926292108	0.5868761842824171	0.1324398472

Table 1.4: ΔE of nearly degenerate energy eigenvalues (a = 9.5, b = 0.5)

value close to that of the top of the hump.

All in all the WKB method does very well. The hardest part seems to be the calculation of the integrals over the momentum, $p(x)$. However, in cases where analytical solutions to the integrals cannot be found, numerical integration may be used. Since numerical integration can be performed with great accuracy, the only penalty we incur is the loss of insight a general solution may have brought.

CHAPTER 2
Flow Equations and Moyal Products

2.1 Overview

The idea behind flow equations [1, 2, 8, 9] for a Hamiltonian is the following. We have some Hamiltonian, H, of which we want to find the eigenvalues. This is done by mapping the original Hamiltonian onto another Hamiltonian with the same spectrum, but which has different eigenvectors. We can achieve this by applying an infinite number of infinitesimal unitary transformations to H in succession. The original Hamiltonian then eventually becomes diagonal (or block diagonal) with respect to the basis which is specified by the new eigenvectors. What is referred to as the flow of the Hamiltonian is the continuous change of H under these transformations.

We therefore have the following situation: H is flowing under an unitary transformation $U(\ell)$ such that for each ℓ,

$$H(\ell) = U^{\dagger}(\ell) H U(\ell) \quad \text{and} \quad H(0) = H \tag{2.1}$$

where ℓ is the flow parameter and $0 \leq \ell < \infty$. These transformations are brought about by the anti-hermitian generator $\eta(\ell)$, where $\eta(\ell)$ is defined by

$$\frac{dU(\ell)}{d\ell} = -U(\ell)\eta(\ell). \tag{2.2}$$

The flow equation to be solved then arises by taking the derivative of $H(\ell)$ with respect

to ℓ:

$$\begin{aligned}
\frac{dH(\ell)}{d\ell} &= \frac{d}{d\ell}\left(U^\dagger(\ell)HU(\ell)\right) \\
&= \frac{dU^\dagger(\ell)}{d\ell}HU(\ell) + U^\dagger(\ell)H\frac{dU(\ell)}{d\ell} \\
&= \frac{dU^\dagger(\ell)}{d\ell}U(\ell)U^\dagger(\ell)HU(\ell) + U^\dagger(\ell)HU(\ell)U^\dagger(\ell)\frac{dU(\ell)}{d\ell} \\
&= \frac{dU^\dagger(\ell)}{d\ell}U(\ell)H(\ell) + H(\ell)U^\dagger(\ell)\frac{dU(\ell)}{d\ell} \\
&= \eta(\ell)H(\ell) - H(\ell)\eta(\ell) \\
&= [\eta(\ell), H(\ell)]. \qquad (2.3)
\end{aligned}$$

In order to obtain results that are consistent, we need to apply the same transformations to the relevant observables and eigenstates. An eigenstate $|\lambda\rangle$, for example, transforms according to

$$|\lambda, \ell\rangle = U^\dagger(\ell)\,|\lambda\rangle\,, \qquad (2.4)$$

while in general an observable A will change in the following fashion:

$$A(\ell) = U^\dagger(\ell)AU(\ell). \qquad (2.5)$$

In the same way as H, its flow equation is given by

$$\frac{dA(\ell)}{d\ell} = [\eta(\ell), A(\ell)]. \qquad (2.6)$$

We can also write down the expectation values of A in term of the transformed observable:

$$\langle\lambda|\,A\,|\lambda\rangle = \langle\lambda|\,U(\ell)U^\dagger(\ell)AU(\ell)U^\dagger\,|\lambda\rangle = \langle\lambda,\ell|\,A(\ell)\,|\lambda,\ell\rangle\,. \qquad (2.7)$$

For H itself, this means that

$$E_n = \langle E_n|\,H\,|E_n\rangle = \langle E_n,\ell|\,H(\ell)\,|E_n,\ell\rangle\,. \qquad (2.8)$$

We shall use this in Chapters 3 and 4 to find the eigenvalues of H once we have determined

$H(\infty)$.

2.2 Choice of generator

2.2.1 Wegner's original generator

In the original work by Wegner [1], the two elements in the commutator that comprised the generator were the diagonal part of the flowing Hamiltonian and the flowing Hamiltonian, $H(\ell)$ itself. In other words,

$$\eta(\ell) = [H_d(\ell), H(\ell)], \tag{2.9}$$

where $H_d(\ell)$ is diagonal in the basis determined by its eigenvectors.

Wegner goes on to show that $H(\ell)$ converges, in the limit of $\ell \to \infty$, to a form that commutes with $H_d(\infty)$, i.e.:

$$[H_d(\infty), H(\infty)] = 0. \tag{2.10}$$

However, later on we use two different generators, whose details we discuss next.

2.2.2 A different choice of generator

A slightly different generator, and one we shall be using later in this work, has the form,

$$\eta(\ell) = [H_0, H(\ell)], \tag{2.11}$$

where H_0 is independent of ℓ. We are essentially free to choose H_0 as we wish, provided it is hermitian. It is relatively simple to show that $H(\ell)$ flows to a form which commutes with H_0 as $\ell \to \infty$. To do this, we make use of the fact that the trace norm is larger than or equal to zero, while it vanishes if and only if its argument vanishes (see Appendix A), as well as the following inequality,

$$\frac{d}{d\ell} tr[(H(\ell) - H_0)^2] = -2tr[[H_0, H(\ell)]^\dagger [H_0, H(\ell)]] < 0. \tag{2.12}$$

This implies that $tr[(H(\ell) - H_0)^2]$ is a monotonically decreasing function of ℓ, which is bounded below by zero. Its derivative must therefore vanish in the $\ell \to \infty$ limit. We

have therefore that $tr[[H_0, H(\ell)]^\dagger [H_0, H(\ell)]]$ must also vanish as ℓ goes to infinity. This is however the trace norm of $\eta(\ell)$, which implies $[H_0, H(\infty)] = 0$, so that H_0 and $H(\infty)$ commute. For a few more mathematical details see Appendix A.

It is important to note that choosing a non-degenerate H_0 will lead to a complete diagonalization of $H(\infty)$. A degenerate H_0 will leave $H(\infty)$ in a block diagonal form. It can also be shown [10] that the eigenvalues of $H(\infty)$ will appear in the same order as those of H_0. This is very useful, since it allows us to find the ground state (or any other excited state for that matter) energy immediately after we have calculated $H(\infty)$ without needing to search through all the eigenvalues (which may be problematic in a numerical calculation where only a few eigenvalues are computed at one time).

2.2.3 Form preserving generator

We now look at a third kind of generator. Whereas Wegner's generator used the diagonal part of the flowing Hamiltonian and the generator described in section 2.2.2 used a fixed operator in the commutator that determines it, the next generator is slightly different. Its purpose is to leave the form of the initial Hamiltonian invariant at any finite ℓ. Where using an η of the form $[H_0, H(\ell)]$ allowed us to control the final point, $H(\infty)$, to which the Hamiltonian would flow, it left us largely in the dark as to the structure of $H(\ell)$ for finite ℓ. It is entirely possible that elements of the matrix of the flowing Hamiltonian become non-zero during the flow [11], even if they are zero in both the initial and final forms. Thus, preserving the structure of the initial Hamiltonian is not only computationally favourable (since fewer new elements are generated), but also intuitively more appealing and allows for a cleaner physical interpretation of what happens during the flow.

In order to construct our form preserving generator, we first introduce a counting operator Q. This operator has integer eigenvalues q_i (generically degenerate) which we will use to label the different subspaces corresponding to different q_i's. If our Hamiltonian has a band block diagonal structure with respect to Q (which is the case we shall be looking at), then the matrix elements $\langle i| H |j\rangle$ vanish whenever $|q_i - q_j| > N$ (for some integer N) for every state $|i\rangle$ and $|j\rangle$ from the subspaces corresponding to q_i and q_j, respectively. Using this definition we see that H does not connect Q-sectors differing by more than N, implying an upper limit on how much H can change Q. Let us assume we can split the Hamiltonian into three parts: a part that leaves Q unchanged and two more which either

increase or decrease Q. We may then write H as

$$H = T_0 + \sum_{n=1}^{N} T_n + \sum_{n=1}^{N} T_{-n} \tag{2.13}$$

$$= T_0 + T_+ + T_-, \quad \text{where} \quad T_+ \equiv \sum_{n=1}^{N} T_n \text{ and } T_- \equiv \sum_{n=1}^{N} T_{-n} \tag{2.14}$$

where T_n is such that it increases Q by n. This is formally written as $[Q, T_n] = nT_n$.

We would like the flow equations to bring H into a form that commutes with Q, that is $[H(\infty), Q] = 0$. This was done in the previous section with the generator $[Q, H(\ell)]$. However, we now require further that the form (2.13) be preserved at each finite ℓ. We therefore require that $H(\ell)$ looks like

$$H(\ell) = T_0(\ell) + \sum_{n=1}^{N} T_n(\ell) + \sum_{n=1}^{N} T_{-n}(\ell), \tag{2.15}$$

where $T_+(\ell) = \sum_{n=1}^{N} T_n(\ell)$ and $T_-(\ell) = \sum_{n=1}^{N} T_{-n}(\ell)$.

It soon becomes apparent though that the generator $\eta(\ell) = [Q, H(\ell)]$ cannot achieve this. To see this, let us consider this generator at $\ell = 0$:

$$\eta(0) = [Q, H] \tag{2.16}$$

$$= [Q, T_0] + \sum_{n=1}^{N} [Q, T_n] + \sum_{n=1}^{N} [Q, T_{-n}] \tag{2.17}$$

$$= \sum_{n=1}^{N} nT_n - \sum_{n=1}^{N} nT_{-n}. \tag{2.18}$$

If we define $\widetilde{T}_+ \equiv \sum_{n=1}^{N} nT_n$ and $\widetilde{T}_- \equiv \sum_{n=1}^{N} nT_{-n}$, the flow equations would then read (also at $\ell = 0$)

$$\left.\frac{\partial H(\ell)}{\partial \ell}\right|_0 = [\widetilde{T}_+ - \widetilde{T}_-, T_0 + T_+ + T_-] \tag{2.19}$$

$$= [\widetilde{T}_+ - \widetilde{T}_-, T_0] + [\widetilde{T}_+, T_+ + T_-] - [\widetilde{T}_-, T_+ + T_-]. \tag{2.20}$$

Since $\widetilde{T}_+$ ($\widetilde{T}_-$) does not commute with T_+ (T_-) we generate terms which can connect Q-sectors up to $2N - 1$ apart, destroying the structure of the initial Hamiltonian. Now it

is clear that $\eta(\ell) = [Q, H(\ell)]$ will not work if our aim is a flowing Hamiltonian with the form of (2.15). However, it is now obvious how $\eta(\ell)$ should be chosen. If we take

$$\eta(\ell) = T_+(\ell) - T_-(\ell), \tag{2.21}$$

then the flow equation becomes

$$\frac{\partial H(\ell)}{\partial \ell} = [T_+(\ell) - T_-(\ell), T_0(\ell)] + 2[T_+(\ell), T_-(\ell)]. \tag{2.22}$$

With $\eta(\ell)$ chosen this way, we see that all the terms which could couple Q-sectors that differ by more than N drop out. It can be shown [12] that choosing the generator this way still produces a final Hamiltonian that conserves Q.

One interesting thing to note is that we could have obtained (2.21) by taking all the coefficients in $\widetilde{T}_+$ and $\widetilde{T}_-$ to be equal to one or, more accurately, by keeping only the overall sign. This is how it is done in [13] and this may be more viable if H cannot easily be written in the form of (2.15).

2.3 Moyal formalism

The second half of this work looks at applications of the flow equation in a Moyal representation [3]. Therefore, in this section we shall look at a few of the details concerning this procedure.

2.3.1 Overview

2.3.1.1 Finite-dimensional case

Let us first consider a finite dimensional Hilbert space and take its dimension to be N. It is possible to define two unitary operators g and h that act irreducibly on the Hilbert space [14, 15]. These operators have the following exchange relation,

$$gh = e^{i\theta} hg. \tag{2.23}$$

Consider now an eigenstate of g. Since g is unitary, its eigenvalue is a phase, say $e^{i\phi}$. Let us see what happens when we let gh act on this eigenstate, $|\phi\rangle$:

$$gh\,|\phi\rangle = e^{i\theta}hg\,|\phi\rangle = e^{i(\phi+\theta)}h\,|\phi\rangle\,. \tag{2.24}$$

We see that $h\,|\phi\rangle$ is therefore also an eigenstate of g. Similarly, so is $h^\dagger\,|\phi\rangle$:

$$gh^\dagger\,|\phi\rangle = h^\dagger hgh^\dagger\,|\phi\rangle = e^{-i\theta}h^\dagger g\,|\phi\rangle = e^{i(\phi-\theta)}h^\dagger\,|\phi\rangle\,. \tag{2.25}$$

We deduce that h and $h^\dagger$ act as ladder operators, raising and lowering ϕ by θ at each application. Furthermore, since g and h act irreducibly, we can reach all the eigenstates of g in the Hilbert space by repeated applications of h or $h^\dagger$.

If we define

$$h^n\,|\phi\rangle = |\phi + n\theta\rangle \equiv |n\rangle\,, \tag{2.26}$$

then

$$g\,|\phi + n\theta\rangle = g\,|n\rangle = e^{i(\phi+n\theta)}\,|n\rangle\,. \tag{2.27}$$

We may set the arbitrarily chosen ϕ to zero without loss of generality.

To find the values that θ may take, we note that $h^\dagger gh = e^{i\theta}g$. We can now take the trace of this equation to obtain

$$\begin{aligned} tr(h^\dagger gh) &= tr(e^{i\theta}g) && (2.28)\\ \Rightarrow tr(ghh^\dagger) &= e^{i\theta}tr(g) && (2.29)\\ \Rightarrow tr(g) &= \sum_{n=0}^{N-1} e^{in\theta} = 0, \quad \text{for } e^{i\theta} \neq 1. && (2.30) \end{aligned}$$

Since

$$\sum_{n=0}^{N-1} e^{in\theta} = \frac{1-e^{iN\theta}}{1-e^{i\theta}}, \tag{2.31}$$

we see that for a non-trivial θ,

$$e^{iN\theta} = 1, \tag{2.32}$$

must hold. From (2.32) we determine that θ must be an integer multiple of $2\pi/N$. It is convenient to choose $\theta = 2\pi/N$, since then the eigenvalues of g are non-degenerate. With this choice, we can define the operators $O(n,m) \equiv g^n h^m$, with $n, m = 0, 1, 2, \ldots N-1$. These operators form a basis on the space of operators on the Hilbert space. To see why this is so, let us take the usual trace inner product of two such operators:

$$\begin{aligned}
(O(n,m), O(n',m')) &= tr[(g^n h^m)^\dagger g^{n'} h^{m'}] = tr[h^{-m} g^{-n} g^{n'} h^{m'}] && (2.33)\\
&= tr[g^{-n} g^{n'} h^{m'} h^{-m}] = \delta_{m',m} tr[g^{n'-n}] && (2.34)\\
&= \delta_{m',m} \sum_{k=0}^{N-1} e^{ik(n'-n)\theta} && (2.35)\\
&= N \delta_{m',m} \delta_{n',n}. && (2.36)
\end{aligned}$$

It is now clear from the above that the operators $O(n,m)$ are linearly independent. Futhermore, noting that there are N^2 of these operators provides simple dimensional grounds to complete the argument for why $O(n,m)$ provides a basis.

We can now write any operator acting on the Hilbert space in terms of this basis in the following way,

$$A = \sum_{n,m=0}^{N-1} c_{n,m} O(n,m) = \sum_{n,m=0}^{N-1} c_{n,m} g^n h^m, \quad \text{where} \quad c_{n,m} = (O(n,m), A)/N. \tag{2.37}$$

Now consider the product of two such operators:

$$\begin{aligned}
AB &= \sum_{n,m=0}^{N-1} \sum_{n',m'=0}^{N-1} c_{n,m} d_{n',m'} g^n h^m g^{n'} h^{m'} && (2.38)\\
&= \sum_{n,m=0}^{N-1} \sum_{n',m'=0}^{N-1} c_{n,m} d_{n',m'} e^{-imn'\theta} g^{n+n'} h^{m+m'}. && (2.39)
\end{aligned}$$

We notice that it appears exactly the same as the product of sums of ordinary scalars, except for the extra phase factor, $e^{-imn'\theta}$. This phase arises due to the way we have chosen

to order our operators g and h. Now for the crux of the matter: We can treat g and h as normal scalars, provided that we incorporate the abovementioned phase when we multiply them. This leads us to write g and h in the following way

$$g \to e^{i\alpha}, \quad h \to e^{i\beta}, \tag{2.40}$$

where g and h are now treated as scalars. Substituting (2.40) into (2.37) we see that it becomes

$$A(\alpha, \beta) = \sum_{n,m=0}^{N-1} c_{n,m} e^{in\alpha} e^{im\beta}. \tag{2.41}$$

Our new product rule is

$$A(\alpha, \beta) * B(\alpha, \beta) = A(\alpha, \beta) e^{i\theta \overleftarrow{\partial}_\beta \overrightarrow{\partial}_\alpha} B(\alpha, \beta), \tag{2.42}$$

where $\overleftarrow{\partial}_\beta$ implies differentiation with respect to β to the left and $\overrightarrow{\partial}_\alpha$ implies differentiation with respect to α to the right. The *-operation is the so-called Moyal product. It can easily be checked that the Moyal product is associative.

2.3.1.2 Infinite-dimensional case

In the case of an infinite dimensional quantum system, we may follow a similar procedure as the one described in the preceding section. We consider for our discussion one particle in one dimension. In this case we start with the following exchange relation,

$$e^{it\hat{p}} e^{is\hat{x}} = e^{i\hbar ts} e^{is\hat{x}} e^{it\hat{p}}, \tag{2.43}$$

where t and s are continuous variables [14, 15]. The operators $\hat{x}$ and $\hat{p}$ are the usual position and momentum operators that obey the canonical commutation relation,

$$[\hat{x}, \hat{p}] = i\hbar. \tag{2.44}$$

We define $O(t, s)$ [16] (similar to $O(n, m)$ above) as $O(t, s) = e^{i\hbar t\hat{p}} e^{i\hbar s\hat{x}}$. Once again, we would like to use the $O(t, s)$ operators as a basis. To show this, we take the trace inner

product:

$$\begin{aligned}(O(t,s),O(t',s')) &= tr[O(t,s)^\dagger O(t',s')] && (2.45)\\ &= \int_{-\infty}^{\infty} dx\, \langle x|\, e^{-is\hat{x}}e^{-it\hat{p}}e^{it'\hat{p}}e^{is'\hat{x}}\, |x\rangle && (2.46)\\ &= \int_{-\infty}^{\infty} dx\, dp\, e^{ix(s'-s)}e^{ip(t'-t)}\frac{e^{ixp/\hbar}}{(2\pi\hbar)^{1/2}}\frac{e^{-ixp/\hbar}}{(2\pi\hbar)^{1/2}} && (2.47)\\ &= \frac{2\pi}{\hbar}\delta(t'-t)\delta(s'-s). && (2.48)\end{aligned}$$

The expansion of a general operator then reads

$$A(\hat{x},\hat{p}) = \int_{-\infty}^{\infty} dt\, ds\, a(t,s)e^{it\hat{p}}e^{is\hat{x}}, \quad \text{where} \quad a(t,s) = \frac{\hbar}{2\pi}(O(t,s),A(\hat{x},\hat{p})). \tag{2.49}$$

If we were now to form the product of two operators, A and B say, we obtain

$$\begin{aligned}A(\hat{x},\hat{p})B(\hat{x},\hat{p}) &= \int_{-\infty}^{\infty} dt\, ds\, dt'\, ds'\, a(t,s)b(t',s')e^{it\hat{p}}e^{is\hat{x}}e^{it'\hat{p}}e^{is'\hat{x}} && (2.50)\\ &= \int_{-\infty}^{\infty} dt\, ds\, dt'\, ds'\, a(t,s)b(t',s')e^{it\hat{p}}e^{it'\hat{p}}e^{is\hat{x}}e^{is'\hat{x}}e^{-i\hbar t's} && (2.51)\\ &= \int_{-\infty}^{\infty} dt\, ds\, dt'\, ds'\, a(t,s)b(t',s')O(t+t',s+s')e^{-i\hbar t's}. && (2.52)\end{aligned}$$

Apart form the factor $e^{-i\hbar t's}$ this is what we would expect to obtain if we had been considering the product of scalar functions. We can therefore conclude that, as above, we may treat A and B as scalar functions under the condition that we introduce a modified product rule which produces the phase $e^{-i\hbar t's}$ correctly. This modified product, the Moyal product, reads,

$$A(x,p) * B(x,p) = A(x,p)e^{i\hbar\overleftarrow{\partial_x}\overrightarrow{\partial_p}}B(x,p). \tag{2.53}$$

Here, as before, $A(x,p)$ and $B(x,p)$ are now scalar functions instead of operators. The non-commutativity of the operators $A(\hat{x},\hat{p})$ and $B(\hat{x},\hat{p})$ is entirely encapsulated by the Moyal product.

In our application of Moyal products and flow equations in the last two chapters, we will find operators that are functions of either $\hat{x}$ or $\hat{p}$ alone. It is therefore instructive to look at the Moyal representation of such operators. Consider $A(\hat{x})$ and its scalar function

counterpart

$$A(x,p) = \int_{-\infty}^{\infty} dt\, ds\, a(t,s) e^{itp} e^{isx}. \tag{2.54}$$

To obtain the representation we first need to calculate $a(t,s)$, which is given by

$$\begin{aligned} a(t,s) &= \frac{\hbar}{2\pi}(O(t,s), A(\hat{x})) = \frac{\hbar}{2\pi} tr[e^{-is\hat{x}} e^{-it\hat{p}} A(\hat{x})] && (2.55)\\ &= \frac{\hbar}{2\pi}\int_{-\infty}^{\infty} dx\ \langle x|\, e^{-is\hat{x}} e^{-it\hat{p}} A(\hat{x})\, |x\rangle && (2.56)\\ &= \frac{1}{(2\pi)^2}\int_{-\infty}^{\infty} dx\, dp\, e^{-isx} e^{-itp} A(x) && (2.57)\\ &= \frac{1}{2\pi}\delta(t)\int_{-\infty}^{\infty} dx\, e^{-isx} A(x). && (2.58) \end{aligned}$$

If we substitute (2.58) into (2.54) we find

$$\begin{aligned} A(x,p) &= \int_{-\infty}^{\infty} dt\, ds\, dx'\, \frac{1}{2\pi}\delta(t) e^{itp} e^{-isx'} e^{isx} A(x') && (2.59)\\ &= e^{ip0}\int_{-\infty}^{\infty} dx'\, \delta(x-x') A(x') && (2.60)\\ &= A(x), && (2.61) \end{aligned}$$

so that the representation of $A(\hat{x})$ is $A(x)$. In other words, if we have an operator that depends only on $\hat{x}$, its Moyal counterpart will be the function where every instance of $\hat{x}$ has been replaced with the number x. In can be shown in a similar fashion that the same holds true for an operator depending only on $\hat{p}$, so that the representation of $A(\hat{p})$ is $A(p)$.

2.3.2 Moyal Bracket Method

We can now combine the functionality of both the Moyal product and flow equations into one. To do this one must first obtain the scalar representations of both the generator and the Hamiltonian (or any other observable one wishes to study). Then any products must be replaced by the Moyal product. In particular the flow equation becomes

$$\frac{\partial H(\ell,\hat{x},\hat{p})}{\partial \ell} = [\eta(\ell,\hat{x},\hat{p}), H(\ell,\hat{x},\hat{p})] \to \frac{\partial H(\ell,x,p)}{\partial \ell} = [\eta(\ell,x,p), H(\ell,x,p)]_*, \tag{2.62}$$

where $[,]_*$ signifies the commutator with respect to the Moyal product,

$$[A, B]_* = A * B - B * A. \tag{2.63}$$

$[,]_*$ is called the Moyal bracket [17].

In general, however, the Moyal product of two operators is very difficult to calculate, since it involves the exponent of differential operators. One can significantly simplify this by making an approximation to first order in $\hbar$ (see (2.53)):

$$A * B \approx AB + i\hbar \frac{\partial A}{\partial x}\frac{\partial B}{\partial p}. \tag{2.64}$$

The corresponding Moyal bracket would be

$$[A, B]_* \approx i\hbar\,(A_x B_p - B_x A_p), \tag{2.65}$$

where subscripts denote partial derivatives. This is a semi-classical approximation, since it is controlled by $\hbar$. This approximation should work well provided that none of the derivatives one has discarded go like powers of $1/\hbar$.

In the case of a generator chosen as in section 2.2.2, one finds the double Moyal bracket involved in the flow equation to be

$$\begin{aligned}
\frac{dH(\ell, x, p)}{d\ell} &= [[H_0, H(\ell, x, p)]_*, H(\ell, x, p)]_* \\
&\approx i\hbar[H_{0_x} H_p - H_x H_{0_p}, H]_* \\
&\approx -\hbar^2[(H_{0_{xx}} H_p + H_{0_x} H_{xp} - H_{0_{xp}} H_x - H_{0_p} H_{xx}) H_p \\
&\qquad -(H_{0_{px}} H_p + H_{0_x} H_{pp} - H_{0_{pp}} H_x - H_{0_p} H_{px}) H_x],
\end{aligned} \tag{2.66}$$

where $A_{xp} \equiv \frac{\partial^2 A}{\partial x \partial p}$. Further corrections can also easily be calculated by keeping successive terms in the Moyal product.

2.4 Quadratic Potentials

In the case of the WKB approximation or a path integral formulation, one finds that one can solve for quadractic potentials exactly. The reason for this is that for these potentials there are no higher order fluctuations in $\hbar$ that are not already included in

the approximation. For example, in the path integral, a quadratic potential leads to a guassian integral of which we know the solution. We now show that the Moyal bracket approach has the same property.

If we take our flowing Hamiltonian to have the form,

$$H(\ell, p, x) = \alpha(\ell)p^2 + \beta(\ell)x^2, \tag{2.67}$$

with

$$\alpha(0) = 1 \tag{2.68}$$
$$\beta(0) = \epsilon > 0, \tag{2.69}$$

and if we take H_0 to be $p^2 + x^2$, then (2.66) (with $\hbar = 1$) becomes a coupled set of two ordinary differential equations:

$$\frac{d\alpha}{d\ell} = -\alpha(\ell)[\alpha(\ell) - \beta(\ell)] \tag{2.70}$$
$$\frac{d\beta}{d\ell} = \beta(\ell)[\alpha(\ell) - \beta(\ell)]. \tag{2.71}$$

The general solutions for α and β are (found using Mathematica's DSolve)

$$\alpha(\ell) = \sqrt{c_1}\tanh(\ell\sqrt{c_1} - c_2\sqrt{c_1}) \tag{2.72}$$
$$\beta(\ell) = \sqrt{c_1}\coth(\ell\sqrt{c_1} - c_2\sqrt{c_1}), \tag{2.73}$$

where c_1 and c_2 are constants of integration.

With initial conditions as specified in (2.68) and (2.69), we find that

$$c_1 = \epsilon \tag{2.74}$$
$$c_2 = -\frac{1}{\sqrt{\epsilon}}\tanh^{-1}(\frac{1}{\sqrt{\epsilon}}). \tag{2.75}$$
$$\tag{2.76}$$

In virtually all cases the exact value of c_2 is irrelevant, however, since we are interested in the $\ell \to \infty$ limit, in which case the tanh and coth terms are both simply 1. We therefore

find that $H(\infty)$ is

$$H(\infty) = \sqrt{\epsilon}(p^2 + x^2), \tag{2.77}$$

and we see that the flow equation simply renormalized the coefficients of H.

There is one case where one must be slightly careful, namely when $H(0) = H_0$. In this case $\epsilon = 1$ and $c_2 = -\infty$. Therefore, $\alpha(\ell)$ and $\beta(\ell)$ remain constant for all ℓ and no flow actually takes place, as is obvious from the flow equation (2.3) with (2.11) as generator. However, this is not really a special case, since, for the harmonic oscillator, (2.77) still holds with $\epsilon = 1$.

We see that the Moyal bracket method, truncated at first order in $\hbar$, also includes the necessary fluctuations to describe quadratic potentials exactly, as is the case for the WKB approximation. This result is of course not very surprising if one notices that (2.66) is exact to all orders in $\hbar$ for quadratic Hamiltonians.

CHAPTER 3
The Quartic Oscillator

3.1 The Model

As our first application of the Moyal bracket method for flow equations, we will look at a harmonic oscillator with an additional quartic interaction in one dimension. This so-called quartic oscillator is often used as a testbed for quantum mechanical approximation. Our Hamiltonian is therefore,

$$H(\hat{p},\hat{x}) = a\hat{p}^2 + b\hat{x}^2 + \lambda\hat{x}^4, \tag{3.1}$$

where $a = \frac{1}{2m}$, $b = \frac{m\omega^2}{2}$, λ controls the strength of the anharmonic interaction and $\hat{x}$ and $\hat{p}$ are the usual position and momentum operators. For this example, we shall only look at cases where $\lambda > 0$. We write H in dimensionless form by scaling $\hat{x} \to \sqrt[4]{\frac{\hbar^2}{m^2\omega^2}}\hat{x}$ and $\hat{p} \to \hbar\sqrt[4]{\frac{m^2\omega^2}{\hbar^2}}\hat{p}$, which gives us

$$H(\hat{p},\hat{x}) = \hat{p}^2 + \hat{x}^2 + \lambda'\hat{x}^4, \tag{3.2}$$

after setting $\hbar, \omega = 1$.

3.2 Flow equations via Moyal brackets

We are interested in finding the eigenvalues of our Hamiltonian. In order to do this with the Moyal bracket approach, we first need to do two things. We need to choose an appropriate generator for the flow equation and we need to convert the generator and the Hamiltonian into their equivalent Moyal formalism representations.

We choose our generator to be in the form discussed in section 2.2.2, where H_0 has been chosen to be the (non-dimensionalized) harmonic oscillator,

$$H_0(\hat{p},\hat{x}) = \hat{p}^2 + \hat{x}^2. \tag{3.3}$$

The eigenstates of H_0 are of course the usual harmonic oscillator states ($|n\rangle$, $n = 0, 1, 2\ldots$),

and the eigenvalues are given by $H_0 |n\rangle = 2(n + \frac{1}{2}) |n\rangle$. Since the spectrum of H_0 is non-degenerate, we expect $H(\infty)$ to be completely diagonal in the harmonic oscillator basis. In addition, the eigenvalues of H will appear in the same order as those of the harmonic oscillator.

We are in the fortunate position that neither H nor H_0 contains terms involving both $\hat{x}$ and $\hat{p}$. We can therefore apply the results of the end of section 2.3.1.2. The respective Moyal representations of these operators will simply be the functions of x and p (as scalars), where $\hat{x}$ has been replaced with x and $\hat{p}$ with p.

With our choice of H_0 we can simplify (2.66) to write down the flow equation in Moyal form (to first order in $\hbar$):

$$\begin{aligned} \frac{\partial H(\ell,p,x)}{\partial \ell} &= [[H_0, H(\ell,p,x)]_*, H(\ell,p,x)]_* && (3.4) \\ &\approx -2[H_x(\ell)(-xH_{pp}(\ell) + pH_{xp}(\ell) + H_x(\ell)) \\ &\quad + H_p(\ell)(xH_{xp}(\ell) - pH_{xx}(\ell) + H_p(\ell))]. && (3.5) \end{aligned}$$

The approximate flow equation can be drastically simplified by a change of variables, namely

$$\begin{aligned} x &= \sqrt{q}\cos(\theta) && (3.6) \\ p &= \sqrt{q}\sin(\theta). && (3.7) \end{aligned}$$

With these new variables, the flow equation becomes

$$\frac{dH(\ell,q,\theta)}{d\ell} \approx 4[H_q(\ell)H_{\theta\theta}(\ell) - H_\theta(\ell)H_{q\theta}(\ell)]. \quad (3.8)$$

It is important to note that this change of variables occurs after we have made the transition to the Moyal representation, where x and p are now simply numbers. Trying to perform this step on the operator level would, if possible, be significantly more complicated. Issues of how the operators should be ordered would have to be taken into account, as well as requiring more complicated Moyal products to be calculated.

One will notice that $H_0(p,x) = p^2 + x^2 = q$. This means that H_0 is independent of θ. Since $H(\ell)$ is flowing to a form that will commute with H_0, we realize that $H(\infty)$ must also be independent of θ and depend only on q. Indeed, (3.8) clearly shows that when

$H(\ell)$ is independent of θ the flow stops and a fixed point has been reached. In a numerical calculation, we may then stop the flow when this convenient condition is satisfied (since integrating all the way to infinity is neither practical nor necessary). One may simply stop when $\frac{\partial H(\ell)}{\partial \theta}$ has become sufficiently small.

3.3 Solving the flow equation

To solve the flow equation we need to provide an initial condition, as is the case for any differential equation. In this case, as already mentioned, $H(0, p, x)$ has the simple form

$$H(0, p, x) = p^2 + x^2 + \lambda' x^4. \tag{3.9}$$

Once again, this is due to the associativity of the Moyal product and the fact that every term in $H(\hat{p}, \hat{x})$ depends only on either $\hat{p}$ or $\hat{x}$ but not both.

Translating to q and θ gives us

$$\begin{aligned} H(0, q, \theta) &= q + \lambda' q^2 \cos^4(\theta) && (3.10) \\ &= q + \lambda' \frac{q^2}{8}(3 + 4\cos(2\theta) + \cos(4\theta)). && (3.11) \end{aligned}$$

The differential equation (3.8) together with the initial condition (3.11) may now be solved. This gives us $H(\ell, q, \theta)$, where, strictly speaking, we need to use the $\ell \to \infty$ limit in calculating eigenvalues. However, in a numerical calculation we cannot integrate all the way to infinity. Therefore integrating until $\frac{\partial H(\ell)}{\partial \theta}$ falls below a chosen tolerance or simply choosing a large enough ℓ to stop at is usually more than sufficient to obtain accurate results.

3.4 Determining the spectrum

To find the eigenvalues of H we turn to equation (2.8). We will, however, need to specifiy $|E_n, \infty\rangle$ in some way. This is done by remembering that the eigenvalues of $H(\infty)$ are ordered in the same way as that of H_0, meaning the n'th excited state of $H(\infty)$ corresponds to the n'th excited state of H_0. This implies that $|E_n, \infty\rangle = |n\rangle$, since $H(\infty)$

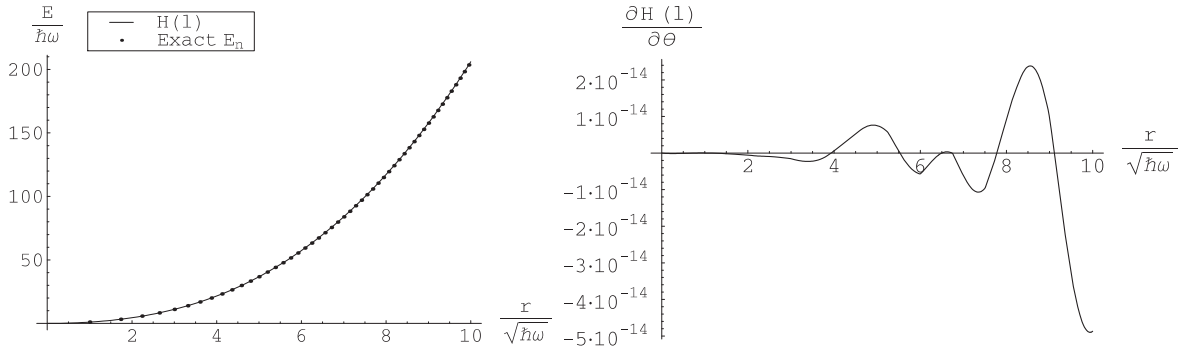

Figure 3.1: (a) First fifty exact eigenvalues for the quartic potential ($\lambda' = 0.1$) together with the flow equation approximation. (b) Derivative of the flowing Hamiltonian, $H(\ell)$, with respect to θ, taken at $\ell = 900$ and $\theta = 0$.

is diagonal in the basis of H_0. Therefore, from (2.8),

$$\begin{aligned} E_n &= \langle E_n | \, H \, | E_n \rangle = \langle E_n, \infty | \, H(\infty) \, | E_n, \infty \rangle \\ &= \langle n | \, H(\infty) \, | n \rangle \, . \end{aligned} \tag{3.12}$$

As pointed out earlier, as $\ell \to \infty$ and $H(\ell)$ becomes diagonal in the basis in which H_0 is, it also becomes a function of q, and thus H_0, only. We can find E_n then by

$$E_n = \langle n | \, H(\infty, H_0) \, | n \rangle = H(\infty, 2n+1), \quad \text{where} \quad n = 0, 1, 2 \ldots . \tag{3.13}$$

In other words, we have replaced each instance of H_0 by its eigenvalue.

3.5 Numerical results

In this section we turn our attention to some numerical results that were obtained for the quartic potential. The reader will notice that most of the graphs are in terms of r $(= \sqrt{q})$ and not q. This is because, although the description of the flow equations is slightly simpler in terms of q, one needs to solve the differential equations on a larger domain when using q. For example, to find the first fifty eigenvalues, one needs to have q span the range $[0, 2(49) + 1 = 99]$, whereas one can find the same number of eigenvalues using r on the range $[0, \sqrt{2(49)+1} \approx 10]$. This allows one to use a finer grid on the space of r and θ (for the same amount of memory), usually leading to an improvement in

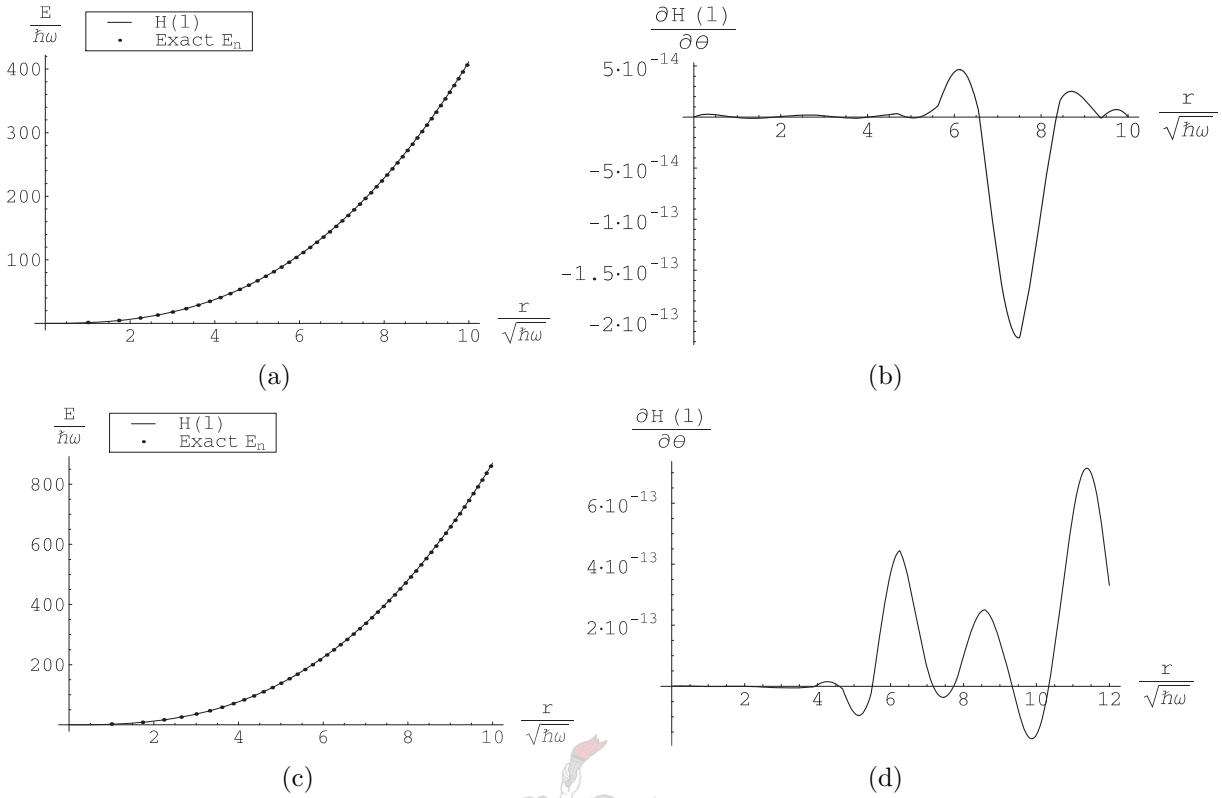

Figure 3.2: (a) First fifty exact eigenvalues for the quartic potential ($\lambda' = 1$) together with the flow equation approximation. (b) Derivative of the flowing Hamiltonian ($\lambda' = 1$), $H(\ell)$, with respect to θ, taken at $\ell = 900$ and $\theta = 0$. (c) Same as (a) except $\lambda' = 10$. (d) Same as in (b) with $\lambda' = 10$.

accuracy. All numerical work was done using Mathematica's built-in numerical differential equation solver, NDSolve.

3.5.1 Numerical eigenvalues

To start off with, we look at the case where λ' is quite small. To be specific, we chose $\lambda' = 0.1$ in our first numerical application of the flow equations to the quartic potential. As one can see in Figure 3.1(a), the flow equation approximation does very well. A relative error of about 2.83% is obtained for the ground state and the error drops to about 0.000481% for the last (50th) eigenvalue shown in this figure. The average (relative) error was 0.0894%, meaning that, on average, we obtain three correct significant digits for each eigenvalue.

As we noted in section 3.3, one may stop integration once $\frac{\partial H(\ell)}{\partial \theta}$ becomes sufficiently

		Exact	WKB	Flow Equations	Relative Error (%)	
					WKB	Flow Eq
λ'=0.1	E_0	1.065285510	1.035155662	1.035098939	2.83	2.83
	E_1	3.306872013	3.285483080	3.285517078	0.647	0.644
	E_2	5.747959269	5.730954235	5.731013951	0.296	0.295
	E_{48}	198.2846571	198.2819353	198.2837052	0.00137	0.0000178
	E_{49}	203.4980353	203.4953503	203.4970574	0.00132	0.0000356
λ'=1	E_0	1.392351642	1.250768760	1.250057196	10.2	10.2
	E_1	4.648812704	4.592560473	4.592609691	1.21	1.21
	E_2	8.655049958	8.613057729	8.613165445	0.485	0.484
	E_{48}	395.4169465	395.4111175	395.4378920	0.00147	0.00530
	E_{49}	406.2009974	406.1952475	406.2222788	0.00142	0.00524
λ'=10	E_0	2.449174072	2.061139563	2.063524463	15.8	15.7
	E_1	8.599003455	8.489468733	8.492548519	1.27	1.23
	E_2	16.63592149	16.54582360	16.54047811	0.542	0.574
	E_{48}	836.8115578	836.7990299	836.0909037	0.00150	0.0861
	E_{49}	859.8370953	859.8247368	858.9498280	0.00144	0.103

Table 3.1: A comparison between the energy eigenvalues obtained via the WKB and flow equations methods

small at some ℓ. The plot 3.1(a) was made by integrating up to $\ell = 1000$. The graph in 3.1(b) shows the derivative $\frac{\partial H(\ell)}{\partial \theta}\Big|_{\ell=900}$. Figure 3.1(b) is a representative plot of the the θ-derivative of $H(\ell)$, showing that it is very small already at $\ell = 900$. Indeed, it is identically zero (to within machine tolerance) at $\ell = 1000$.

Figures 3.2(a) and 3.2(c) show the results obtained for a slightly larger ($\lambda' = 1$) and much larger ($\lambda' = 10$) value of λ'. As one can see, the flow equations do almost equally well in all three cases (average relative errors: $\lambda' = 1$: 0.258%, $\lambda' = 10$: 0.395%), no matter the strength of the coupling constant λ'. This is a property that a perturbative approximation does not share.

3.5.1.1 Comparison with the WKB method

To end this chapter, we shall make a brief comparison between the energy eigenvalues obtained from the WKB approximation and the flow equations. Table 3.1 lists the first, second, third, 49th and 50th energy eigenvalues obtained numerically by direct diagonalization (Exact) (see section 1.2.2), the WKB approximation (WKB) and the flow equations for the three values of λ' we have mentioned before, namely $\lambda' = 0.1, 1, 10$.

For all these values of λ' we see that the flow equations achieve comparable or marginally better accuracy in the ground state and first excited state. For the smallest value of λ' the flow equations do better across all the eigenvalues. For larger λ', they start to do slightly worse until for $\lambda' = 10$ the flow equations lose to the WKB method by two orders of magnitude in the accuracy of the 50th eigenvalue. However, this is at least partly due to finite size and edge effects which almost always plague numerical solutions of PDEs.

We can summarize by saying, that from what we have seen so far, the Moyal bracket method compares favourably indeed with the WKB approximation.

CHAPTER 4
The Symmetric Double-Well Potential

4.1 The Model

In the previous chapter we applied our method of flow equations in the context of Moyal products and brackets to the quartic oscillator. In this chapter we shall keep the quartic term, but add an additional quadratic term with a negative sign, to give us the symmetric double-well (SDW) potential. One of the interesting things about this potential is the fact that tunneling can now occur between the two wells, lifting the degeneracy one expects classically (since the wells have the same shape). This shift in energy is very small at the ground state, but increases towards the top of the centre hump in the potential. It is of particular interest to be able to calculate this level splitting, since it is a truly non-perturbative effect. We consider a potential as in section 1.2, in other words,

$$H(\hat{p},\hat{x}) = \hat{p}^2 + (1+\epsilon)\hat{x}^2 + \lambda\hat{x}^4. \tag{4.1}$$

We consider only positive λ and negative ϵ (in fact $\epsilon < -1$ is of course required to form two wells) and have written $H(\hat{p},\hat{x})$ in dimensionless form already.

4.2 Flow Equations

To set up the flow equations for the symmetric double-well potential, we would like to proceed just as in section 3.2 and have H flow to a form that commutes with the harmonic oscillator

$$H_0(\hat{p},\hat{x}) = \hat{p}^2 + \hat{x}^2, \tag{4.2}$$

with eigenstates and -values just as described in section 3.2.

We would like to, once again, construct the Moyal representations of the various operators (which is still trivial, considering that no operator contains terms which have mixtures of $\hat{x}$ and $\hat{p}$) and transform the resulting operator and flow equation to functions of q and θ as we did in section 3.2, by using (3.6) and (3.7).

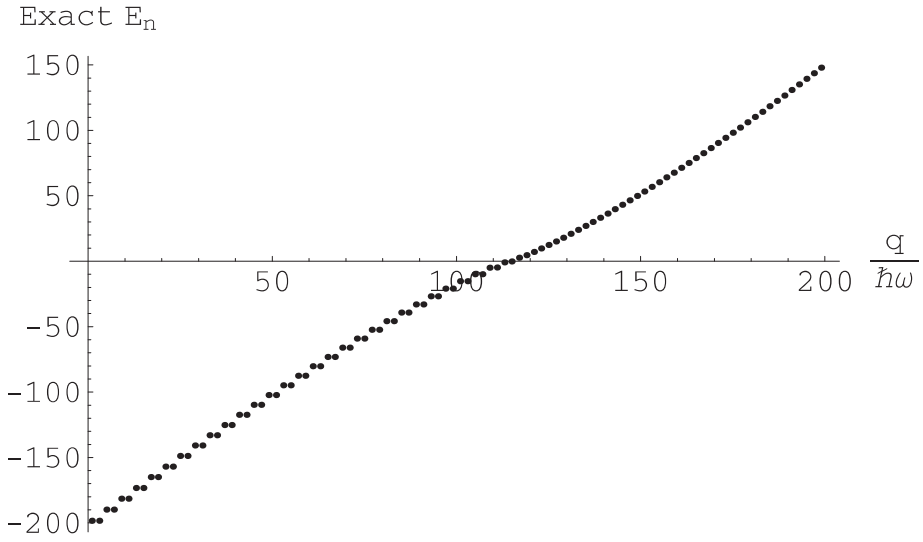

Figure 4.1: First hundred exact eigenvalues for the SDW potential with $\epsilon = -10$ and $\lambda = 0.1$

However, if one were to look at a plot (Figure 4.1) of the actual eigenvalues (obtained by direct diagonalization of the matrix of H truncated at 1000×1000) of this potential as a function of q, one immediately sees a problem. The function $H(\infty, q)$ one would have to obtain to produce accurate results would have to contain a series of steps to produce the correct eigenvalues in the part where the eigenvalues are negative. This, however, implies that derivatives of $H(\ell)$ would start to be of the order of $1/\hbar$ which would render our first order expansion invalid. A more mathematical argument would be that the energy splitting is exponentially small and has a $e^{-1/\hbar}$ behaviour from which one can immediately see that the derivatives become of order $1/\hbar$ [4, 18, 19]. We are somewhat fortunate, therefore, that we can circumvent this problem. To see how this is possible, let us look at the Hamiltonian when written in terms of creation and annihilation operators laddering between the eigenstates of H_0:

$$\begin{aligned} H(a^\dagger, a) &= (2\hat{n}+1) + \frac{\epsilon}{2}(aa + a^\dagger a^\dagger + 2\hat{n} + 1) \\ &\quad + \frac{\lambda}{4}[aaaa + a^\dagger a^\dagger a^\dagger a^\dagger + 2(2\hat{n}+3)aa + 2a^\dagger a^\dagger(2\hat{n}+3) \\ &\quad + (\hat{n}+2)(\hat{n}+1) + \hat{n}(\hat{n}-1) + (2\hat{n}+1)^2]. \end{aligned} \tag{4.3}$$

Here we have used the following substitutions,

$$\hat{x} = \frac{1}{\sqrt{2}}(a + a^\dagger) \tag{4.4}$$

$$\hat{p} = \frac{1}{i\sqrt{2}}(a - a^\dagger) \tag{4.5}$$

$$\hat{n} = a^\dagger a \tag{4.6}$$

to transform (4.1) into (4.3). It is clear from (4.3) that, when H is applied to the harmonic oscillator basis states, we create new states with quantum number n that only differ from the original state by zero, two or four. This implies that we can subdivide the states into an even and an odd subspace, where H never mixes the two together. This allows us to construct flow equations on the even and odd sectors separately, each with different initial conditions. To ensure that we do not create, during the flow, a Hamiltonian that does mix the different sectors, we shall be using a generator that preserves the form of the Hamiltonian at each finite ℓ, as described in section 2.2.3. In this case, our harmonic oscillator H_0 will play the role of the counting operator Q. This allows us to construct a flow equation that preserves the form of H and will eventually lead to a $H(\infty)$ which commutes with H_0 at the same time.

In order to determine the flow equations, we need to know the form of the initial Hamiltonian in each subspace. This is what we will derive next.

4.3 Initial conditions

In order to find the initial conditions, we first construct a mapping from the harmonic oscillator states of H_0, as defined in (4.2), to the basis states of a new harmonic oscillator. To make this statement more explicit, we want to map

$$\text{old basis} \quad \begin{cases} \text{even:} & |2n\rangle \\ \text{odd:} & |2n+1\rangle \end{cases} \quad \rightarrow |n\rangle \text{ new basis}, \quad n = 0, 1, 2, 3, \ldots \tag{4.7}$$

Together with these new states, we introduce new operators B and $B^\dagger$ which act on the $|n)$ in the usual way,

$$B^\dagger |n) = \sqrt{n+1}\,|n+1) \tag{4.8}$$
$$B\,|n) = \sqrt{n}\,|n-1)\,. \tag{4.9}$$

In order to write H in term of these new operators, we need to find how B and $B^\dagger$ depend on a and $a^\dagger$.

We start by noting that if $B^\dagger$ raises n by one in the new basis, the original basis state will need to be raised by two in order to keep the subspaces separate. We first look at the even sector. We need an operator that raises $|2n\rangle$ by two. This operator will obviously need to contain a factor of $a^\dagger a^\dagger$ in it. However, this is not enough on its own, since

$$a^\dagger a^\dagger |2n\rangle = \sqrt{2n+1}\sqrt{2n+2}\,|2n+2\rangle = \sqrt{2n+1}\sqrt{2n+2}\,|n+1) \tag{4.10}$$
$$\neq B^\dagger |n) = \sqrt{n+1}\,|n+1)\,. \tag{4.11}$$

We therefore need to add a factor to $a^\dagger a^\dagger$ that will correct the prefactors. If we therefore take this new operator to be $\frac{1}{\sqrt{2\hat{n}-2}}\,a^\dagger a^\dagger$, we see that

$$\frac{1}{\sqrt{2\hat{n}-2}}\,a^\dagger a^\dagger |2n\rangle = \frac{\sqrt{2n+1}\sqrt{2n+2}}{\sqrt{2(2n+2)-2}}\,|2n\rangle = \sqrt{n+1}\,|2n+2\rangle \tag{4.12}$$
$$= \sqrt{n+1}\,|n+1) = B^\dagger |n)\,, \tag{4.13}$$

so that we need to associate

$$B^\dagger = \frac{1}{\sqrt{2\hat{n}-2}}\,a^\dagger a^\dagger \tag{4.14}$$
$$B = aa\frac{1}{\sqrt{2\hat{n}-2}} \tag{4.15}$$
$$\hat{N} = B^\dagger B = \frac{\hat{n}}{2}, \tag{4.16}$$

where $\hat{n} = a^\dagger a$. These new operators also obey the standard commutator for creation and

annihilation operators:

$$\begin{aligned}
[B, B^\dagger] &= aaf(\hat{n})^2 a^\dagger a^\dagger - f(\hat{n}) a^\dagger a^\dagger aaf(\hat{n}) \\
&= (\hat{n}+1)(\hat{n}+2) f(\hat{n}+2)^2 - \hat{n}(\hat{n}-1) f(\hat{n})^2 \\
&= \frac{(\hat{n}+1)(\hat{n}+2)}{2(\hat{n}+1)} - \frac{\hat{n}(\hat{n}-1)}{2(\hat{n}-1)} \\
&= 1, \qquad (4.17)
\end{aligned}$$

where $f(\hat{n}) = 1/\sqrt{2\hat{n}-2}$.

For the odd sector we can do similar calculations to arrive at the following associations:

$$B^\dagger = \frac{1}{\sqrt{2\hat{n}}} a^\dagger a^\dagger \qquad (4.18)$$

$$B = aa \frac{1}{\sqrt{2\hat{n}}} \qquad (4.19)$$

$$\hat{N} = B^\dagger B = \frac{\hat{n}-1}{2} \qquad (4.20)$$

$$[B, B^\dagger] = 1. \qquad (4.21)$$

By reversing equations (4.14) to (4.16) and (4.18) to (4.20) we find the following relations for $a^\dagger a^\dagger$ and aa in terms of $B^\dagger$ and B:

Even:

$$a^\dagger a^\dagger = \sqrt{4\hat{N}-2}\, B^\dagger \qquad (4.22)$$

$$aa = B\sqrt{4\hat{N}-2} \qquad (4.23)$$

$$\hat{n} = 2\hat{N}, \qquad (4.24)$$

Odd:

$$a^\dagger a^\dagger = \sqrt{4\hat{N}+2}\, B^\dagger \qquad (4.25)$$

$$aa = B\sqrt{4\hat{N}+2} \qquad (4.26)$$

$$\hat{n} = 2\hat{N}+1. \qquad (4.27)$$

Equations (4.22) to (4.24) and (4.25) to (4.27) may then be substituted into (4.3) to obtain

the initial Hamiltonians for the even and odd subspaces respectively:

$$\begin{aligned} H_E(B,B^\dagger) &= (4\hat{N}+1)+\frac{\epsilon}{2}\left(B\sqrt{4\hat{N}-2}+\sqrt{4\hat{N}-2}\,B^\dagger+4\hat{N}+1\right) \\ &\quad +\frac{\lambda}{4}\Big[B\sqrt{4\hat{N}-2}B\sqrt{4\hat{N}-2}+\sqrt{4\hat{N}-2}\,B^\dagger\sqrt{4\hat{N}-2}\,B^\dagger \\ &\quad +2B\sqrt{4\hat{N}-2}+4B\sqrt{4\hat{N}-2}\hat{N}+4\hat{N}B\sqrt{4\hat{N}-2} \\ &\quad +2\sqrt{4\hat{N}-2}\,B^\dagger+4\sqrt{4\hat{N}-2}\,B^\dagger\hat{N}+4\hat{N}\sqrt{4\hat{N}-2}\,B^\dagger \\ &\quad +(2\hat{N}+2)(2\hat{N}+1)+2\hat{N}(2\hat{N}-1)+(4\hat{N}+1)^2\Big] \qquad (4.28) \\ H_O(B,B^\dagger) &= (4\hat{N}+3)+\frac{\epsilon}{2}\left(B\sqrt{4\hat{N}+2}+\sqrt{4\hat{N}+2}\,B^\dagger+4\hat{N}+3\right) \\ &\quad +\frac{\lambda}{4}\Big[B\sqrt{4\hat{N}+2}B\sqrt{4\hat{N}+2}+\sqrt{4\hat{N}+2}\,B^\dagger\sqrt{4\hat{N}+2}\,B^\dagger \\ &\quad +2B\sqrt{4\hat{N}+2}+2B\sqrt{4\hat{N}+2}(2\hat{N}+1)+2(2\hat{N}+1)B\sqrt{4\hat{N}+2} \\ &\quad +2\sqrt{4\hat{N}+2}\,B^\dagger+2\sqrt{4\hat{N}+2}\,B^\dagger(2\hat{N}+1)+2(2\hat{N}+1)\sqrt{4\hat{N}+2}\,B^\dagger \\ &\quad +(2\hat{N}+3)(2\hat{N}+2)+(2\hat{N}+1)(2\hat{N})+(4\hat{N}+3)^2\Big], \qquad (4.29) \end{aligned}$$

where H_E and H_O denote the initial Hamiltonians in the even sector and odd sector respectively.

Our next step will be to find the Moyal representations of H_E and H_O (see Appendix B for the exact initial conditions). This process is made quite complicated by having to find the representations of the square roots which appear in both H_E and H_O. However, we can find them to lowest order quite easily. First, we note that

$$\begin{aligned} B^\dagger &= \frac{1}{\sqrt{2}}(\hat{X}-i\hat{P}) \qquad (4.30) \\ B &= \frac{1}{\sqrt{2}}(\hat{X}+i\hat{P}) \qquad (4.31) \\ \hat{N} &= B^\dagger B=\frac{1}{2}(\hat{P}^2+\hat{X}^2-1). \qquad (4.32) \end{aligned}$$

Each of these have Moyal representations where $\hat{X}$ and $\hat{P}$ are simply replaced by their corresponding number. It would therefore also be trivial to find the Moyal form of the square of the square roots. Letting $M(\cdot)$ indicate the Moyal representation of some operator, we

have that to lowest order in the Moyal product,

$$M(f^2) = M(f) * M(f) \overset{\text{lowest order}}{=} M(f)M(f) \tag{4.33}$$

$$\Rightarrow \quad M(f) = \sqrt{M(f^2)}. \tag{4.34}$$

In this way we see that the Moyal representations of the square roots are

$$\text{Even:} \qquad \sqrt{4\hat{N} - 2} \to \sqrt{2[(P^2 + X^2) - 2]} \tag{4.35}$$

$$\text{Odd:} \qquad \sqrt{4\hat{N} + 2} \to \sqrt{2[P^2 + X^2]}. \tag{4.36}$$

We can now substitute (4.35) into (4.28) and (4.36) into (4.29), which, together with the Moyal forms of $B^\dagger$ and B, gives us the initial Hamiltonians in terms of X and P. After some simplification and once again transforming to q and θ, we obtain the initial conditions for the even and odd sectors respectively,

$$\begin{aligned} H_E(q,\theta) &= \frac{1}{4}\left[-4 - 2\epsilon + \lambda + 2(4 + 2\epsilon - 4\lambda + 3\lambda q)q \right. \\ &\quad +4\left((\epsilon - \lambda)\sqrt{(q-2)q} + 2\lambda\sqrt{(q-2)q}\; q\right)\cos(\theta) \\ &\quad \left. +2\lambda(q-2)q\cos(2\theta)\right] \end{aligned} \tag{4.37}$$

$$\begin{aligned} H_O(q,\theta) &= \frac{1}{4}\left[4 + 2\epsilon + \lambda + 2(4 + 2\epsilon + 2\lambda + 3\lambda q)q \right. \\ &\quad +4(\epsilon + \lambda + 2\lambda q)q\cos(\theta) \\ &\quad \left. 2\lambda q^2\cos(2\theta)\right]. \end{aligned} \tag{4.38}$$

From (4.37) and (4.38) it is clear that in both the even and odd sectors, the initial Hamiltonian has the following structure,

$$H(0,q,\theta) = n_0(0,q) + n_1(0,q)\cos(\theta) + n_2(0,q)\cos(2\theta). \tag{4.39}$$

However, we cannot easily use this form to get our generator, since both $\cos(\theta)$ and $\cos(2\theta)$ contain terms that both increase and decrease q. To separate these parts, we first note

that

$$B^\dagger \rightarrow \frac{1}{\sqrt{2}}(X - iP) = \sqrt{\frac{q}{2}}e^{-i\theta} \tag{4.40}$$

$$B \rightarrow \frac{1}{\sqrt{2}}(X + iP) = \sqrt{\frac{q}{2}}e^{i\theta}, \tag{4.41}$$

so that the $e^{-i\theta}$ part in $\cos(\theta)$ increases q and the $e^{i\theta}$ part decreases it. Therefore,

$$H(\ell, q, \theta) = n_0(\ell, q) + n_1(\ell, q)\left(\frac{1}{2}e^{i\theta} + \frac{1}{2}e^{-i\theta}\right) + n_2(\ell, q)\left(\frac{1}{2}e^{2i\theta} + \frac{1}{2}e^{-2i\theta}\right) \tag{4.42}$$

$$= \underbrace{n_0(\ell, q)}_{T_0(\ell)} + \underbrace{\left(n_1(\ell, q)\frac{1}{2}e^{-i\theta} + n_2(\ell, q)\frac{1}{2}e^{-2i\theta}\right)}_{T_+(\ell)} + \underbrace{\left(n_1(\ell, q)\frac{1}{2}e^{i\theta} + n_2(\ell, q)\frac{1}{2}e^{2i\theta}\right)}_{T_-(\ell)}. \tag{4.43}$$

According to what we learned in section 2.2.3, we should now take our generator to be

$$\eta(\ell) = T_+(\ell) - T_-(\ell) = -i(n_1(\ell, q)\sin(\theta) + n_2(\ell, q)\sin(2\theta)). \tag{4.44}$$

We can now finally find our flow equations (which is the same in both sectors) by using (4.44) and (4.39) in our Moyal brackets to first order. After grouping terms we obtain three equations. One for n_0, n_1 and n_2 repectively,

$$\frac{\partial n_0}{\partial \ell} = -\frac{1}{2}\frac{\partial n_1^2}{\partial q} - \frac{\partial n_2^2}{\partial q} \tag{4.45}$$

$$\frac{\partial n_1}{\partial \ell} = -n1(\ell, q)\frac{\partial n0}{\partial q} - 2n2(\ell, q)\frac{\partial n1}{\partial q} - n1(\ell, q)\frac{\partial n2}{\partial q} \tag{4.46}$$

$$\frac{\partial n_2}{\partial \ell} = -2n2(\ell, q)\frac{\partial n_0}{\partial q}, \tag{4.47}$$

with corresponding initial conditions:

Even:

$$n_0(0,q) = \frac{1}{4}(-4-2\epsilon+\lambda+2(4+2\epsilon-4\lambda+3\lambda q)q) \tag{4.48}$$
$$n_1(0,q) = (\epsilon-\lambda)\sqrt{(q-2)q}+2\lambda\sqrt{(q-2)q}\,q \tag{4.49}$$
$$n_2(0,q) = \frac{1}{2}\lambda(q-2)q, \tag{4.50}$$

Odd:

$$n_0(0,q) = \frac{1}{4}(4+2\epsilon+\lambda+2(4+2\epsilon+2\lambda+3\lambda q)q) \tag{4.51}$$
$$n_1(0,q) = (\epsilon+\lambda+2\lambda q)q \tag{4.52}$$
$$n_2(0,q) = \frac{1}{2}\lambda q^2. \tag{4.53}$$

If one expands these initial conditions in orders of $\hbar$, one sees that they are the same to lowest order. If one wishes to calculate the level splitting, for example, one needs to calculate the first (and higher) order correction in each sector and subtract them from each other.

4.4 Eigenvalues

As we saw in section 2.2.3, the flow equations derived above preserve the form of the Hamiltonian, while still ensuring that $H(\ell)$ converges to a form that commutes with H_0 in the $\ell \to \infty$ limit. For each sector $H_0 = 2\hat{N}+1$ (operator) or $H_0 = q$ (scalar). Since, once again, $H(\infty)$ must be independent of θ, we have that $n_1(\infty,q) = 0 = n_2(\infty,q)$. This implies $H(\infty,q) = n_0(\infty,q)$, so that, similar to section 3.4, we can find the eigenvalues E_n of H in the following way

$$E_n = H(\infty, 2N+1) = n_0(\infty, 2N+1). \tag{4.54}$$

Once we have calculated the energies in each sector, we can find the level splitting for the nearly-degenerate eigenvalues by subtracting those in the even sector (the smaller of the two) from those in the odd sector.

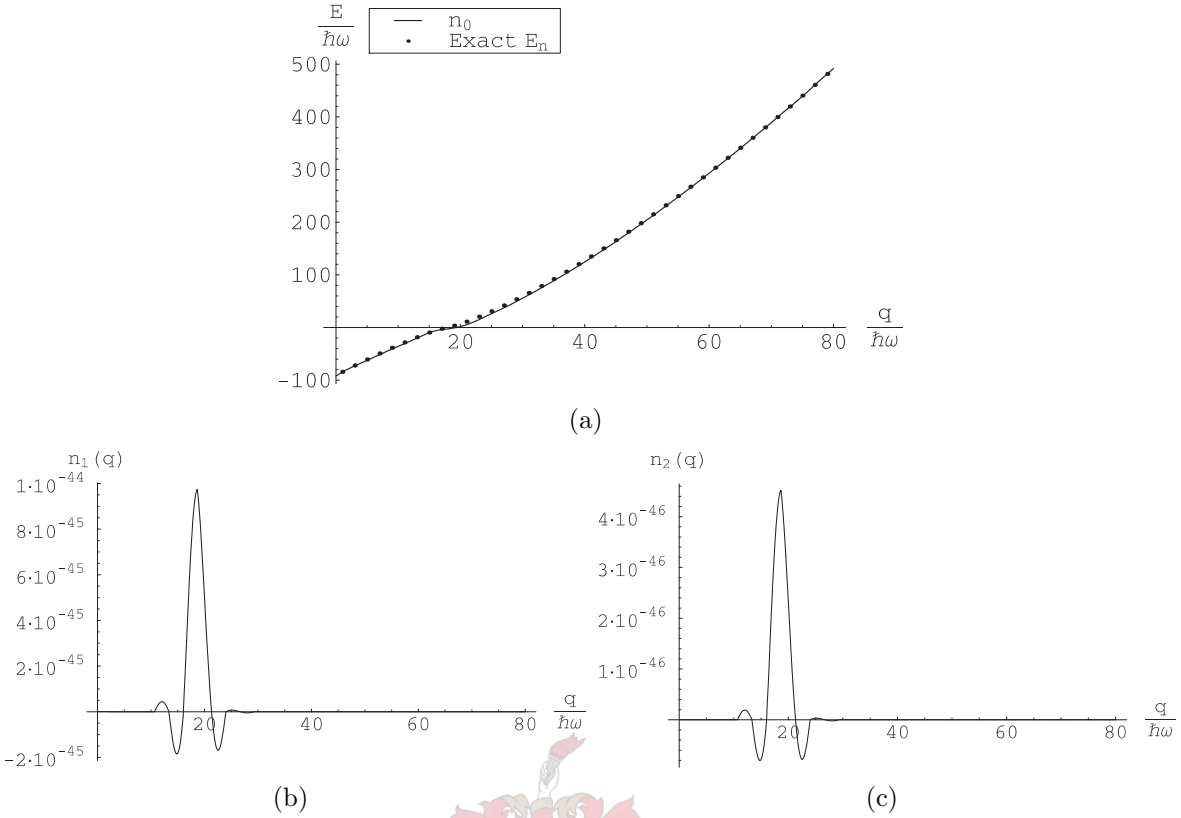

Figure 4.2: (a) First forty exact even eigenvalues for the SDW potential ($\epsilon = -20$, $\lambda' = 1$) together with the flow equation approximation ($n_0(10000, q)$). (b) $n_1(10000, q)$. (c) $n_2(10000, q)$

4.5 Numerical results and comparison with the WKB method

It proved to be quite difficult to obtain accurate numerical results for the SDW potential. The flow equation for n_0 was very sensitive to where the integration for q ended, often veering sharply off-course near the middle of the q domain. However, despite these difficulties, we still do quite well, though not as well as we have seen the WKB method do in chapter 1.

4.5.1 Numerical spectrum

Figure 4.2 shows us a typical result when solving for the eigenvalues of the SDW potential using the techniques and approximations described in this chapter. The relative errors of eigenvalues below the hump are generally on the order of a few percent. Above the hump we do much better, with errors dropping to below 1%. For the fortieth eigenvalue accuracy had improved to such an extent that the relative error was only 0.0186%.

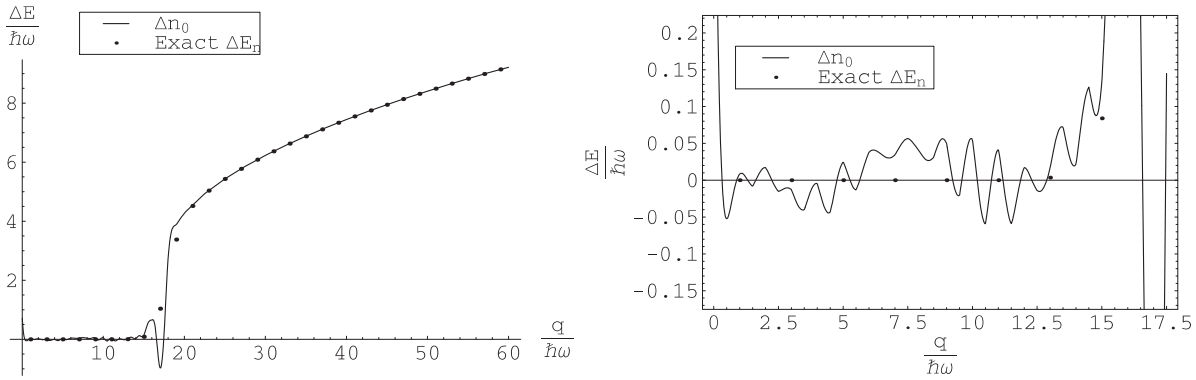

(a) (b)

Figure 4.3: (a) First thirty exact energy differences for the SDW potential ($\epsilon = -20$, $\lambda' = 1$) together with the Moyal bracket approximation difference. (b) Close up of the region $q \in [0, 17.5]$

Generally speaking, the accuracy is worse for the SDW potential than for the quadratic potential. It is therefore ironic that we obtain the ground state energy of this SDW potential with a relative error of 0.386%, which is almost an order of magnitude smaller than even that of the quartic potential with $\lambda' = 0.1$. Why this is so is not entirely clear at the time of writing. Over the first forty eigenvalues, the flow equations give an average relative error of 4%, whereas the WKB method achieves a slightly better 2.28%. One cannot help but note the very sharp spike near $q = 20$ in the graphs of 4.2(b) and 4.2(c). This is where the eigenvalues switch from negative to positive, or put a different way, where the total energy of the particle in the potential goes from being smaller than that of the centre hump to being larger. This phenomenon occurs for all values of ϵ and λ as long as there is at least one eigenvalue smaller than the hump. This goes hand in hand with a very significant decrease in accuracy, where the relative error typically rises to near or above 100%. This corresponds to an increase of about two orders of magnitude in the relative error. Comparatively, the relative error made by the WKB method rises only about one order of magnitude in the same region. Both methods recover once the hump is cleared.

4.5.2 Numerical level splitting

Unfortunately it was not possible at the time of writing to obtain sufficiently accurate numerical results to show conclusively that the Moyal bracket method could (or could not) calculate this level splitting. We see in Figure 4.3(a) that the Moyal bracket method

exibits the desired general behaviour. However, from Figure 4.3(b), which shows a zoomed in view of the region where the eigenvalues are almost degenerate, it is clear that the energy splitting calculated this way is not reliable due to large numerical oscillations. The WKB results for the level splitting can be seen in Table 1.4.

It is clear therefore that work needs to be done to improve accuracy, so that a conclusive statement can be made either way as to whether we may use the Moyal bracket method to calculate the split in energy.

Conclusion

From what we have seen about the semi-classical approximation to the flow equations, it is clear that they measure up quite well when compared to the WKB method.

In the treatment of the quartic oscillator with the Moyal bracket method, we saw that we could get marginally better results for the eigenvalues of the lowest states, though it appears that accuracy improves somewhat slower than WKB method as the energy increases.

The symmetric double-well potential provided a much greater challenge to the flow equations. In order to ensure that the initial conditions were smooth enough for our expansion in $\hbar$ to work, we had to separate the even and the odd subspaces; a procedure not without its own difficulties. The resulting PDEs were far less stable numerically and it took some effort to produce reliable results. Furthermore, these results need to be improved to enable the calculation of the level splitting, something which was not possible at the writing of this thesis.

Despite these problems, the Moyal bracket method remains straight-forward to implement with the greatest challenge lying in finding initial conditions which are sufficiently smooth for our approximation to remain valid. Furthermore, the non-perturbative nature of our approximation enables us to apply it in situations where a perturbative expansion would fail (as with the SDW potential). It therefore seems probable that the Moyal bracket approach will find use in other situations where a semi-classical approximation would be applicable.

APPENDIX A
Diagonality or block diagonality of $H(\infty)$

With our choice of generator as $\eta(\ell) = [H_0, H(\ell)]$, we obtain the following flow equation:

$$\frac{dH(\ell)}{d\ell} = [[H_0, H(\ell)], H(\ell)]. \tag{A.1}$$

We consider now the following derivative,

$$\begin{aligned}
\frac{d}{d\ell} tr[(H(\ell) - H_0)^2] &= \frac{d}{d\ell} tr[H(\ell)^2 - H(\ell)H_0 - H_0 H(\ell) + H_0^2] && \text{(A.2)}\\
&= tr[\frac{dH(\ell)}{d\ell} H(\ell) - H(\ell)\frac{dH(\ell)}{d\ell} - \frac{dH(\ell)}{d\ell} H_0 - H_0 \frac{dH(\ell)}{d\ell}] && \text{(A.3)}\\
&= tr[2(H(\ell) - H_0)\frac{dH(\ell)}{d\ell}] && \text{(A.4)}\\
&= 2tr[(H(\ell) - H_0)[[H_0, H(\ell)], H(\ell)]] && \text{(A.5)}
\end{aligned}$$

where we have used the cyclic permutability of operators in a trace in the second last line.

We now look at the two terms in (A.5) separately. Firstly,

$$\begin{aligned}
tr(H(\ell)[[H_0, H(\ell)], H(\ell)]) &= tr(H(\ell)[[H_0, H(\ell)]H(\ell) - H(\ell)[H_0, H(\ell)]]) && \text{(A.6)}\\
&= tr(H(\ell)^2[H_0, H(\ell)] - H(\ell)^2[H_0, H(\ell)]) && \text{(A.7)}\\
&= 0. && \text{(A.8)}
\end{aligned}$$

Secondly,

$$\begin{aligned}
tr(H_0[[H_0, H(\ell)], H(\ell)]) &= tr(H_0[[H_0, H(\ell)]H(\ell) - H(\ell)[H_0, H(\ell)]]) && \text{(A.9)}\\
&= tr(H(\ell)H_0[H_0, H(\ell)] - H_0 H(\ell)[H_0, H(\ell)]) && \text{(A.10)}\\
&= tr([H(\ell), H_0][H_0, H(\ell)]) && \text{(A.11)}\\
&= tr([H_0, H(\ell)]^\dagger[H_0, H(\ell)]). && \text{(A.12)}
\end{aligned}$$

Substituting (A.8) and (A.12) back into (A.5) we find,

$$\frac{d}{d\ell} tr[(H(\ell) - H_0)^2] = -2tr[[H_0, H(\ell)]^\dagger[H_0, H(\ell)]] < 0 \quad (= 0 \text{ iff } [H_0, H(\ell)] = 0). \tag{A.13}$$

Since $tr[(H(\ell)-H_0)^2] > 0$, we see that it is a monotomically decreasing function of ℓ which is bounded below by zero. Therefore, its derivative must vanish in the limit of $\ell \to \infty$. This implies that $tr[[H_0, H(\ell)]^\dagger [H_0, H(\ell)]]$ must also vanish for $\ell \to \infty$. If one introduces the concept of a trace norm defined by

$$\text{Norm}(A) = tr[A^\dagger A], \tag{A.14}$$

one sees that $tr[[H_0, H(\ell)]^\dagger [H_0, H(\ell)]]$ is exactly the trace norm of $[H_0, H(\ell)]$. It can easily be shown that the trace norm satisfies the conditions for being a norm, such as positive definiteness amongst others. This, together with $tr[[H_0, H(\infty)]^\dagger [H_0, H(\infty)]] = 0$, implies that $[H_0, H(\infty)] = 0$.

Let $|n\rangle$ be an eigenstate of H_0 with eigenvalue λ_n, then

$$\begin{aligned} 0 &= \langle n| \left[H_0, H(\infty)\right] |m\rangle = \langle n| \, H_0, H(\infty) - H(\infty) H_0 \, |m\rangle & \text{(A.15)} \\ &= (\lambda_n - \lambda_m) \langle n| \, H(\infty) \, |m\rangle \, . & \text{(A.16)} \end{aligned}$$

Therefore, if H_0 is non-degenerate, we find that $H(\infty)$ is diagonal, and if H_0 is degenerate $H(\infty)$ has a block diagonal structure.

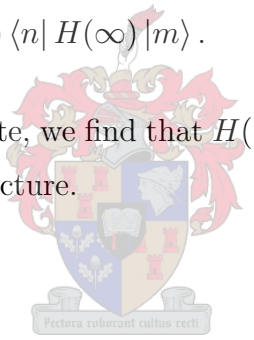

APPENDIX B
Exact initial conditions for the SDW potential

In section 4.3 we derived the flow equations and initial conditions for the SDW potential that preserve the form of the Hamiltonian during flow for the even and odd subpaces of H respectively. It was also done only to lowest order in the Moyal product. We now derive the exact Moyal representation of the above to all orders of $\hbar$.

We start out with the operator equalities for $a^\dagger a^\dagger$, $a^\dagger a^\dagger a^\dagger a^\dagger$, $\hat{n}$ and their hermitian conjugates for the even and odd subspaces:

Even:

$$a^\dagger a^\dagger = \sqrt{4\hat{N} - 2}B^\dagger \tag{B.1}$$

$$aa = \sqrt{4\hat{N} + 2}B \tag{B.2}$$

$$a^\dagger a^\dagger a^\dagger a^\dagger = \sqrt{4\hat{N} - 2}\sqrt{4\hat{N} - 6}B^\dagger B^\dagger \tag{B.3}$$

$$aaaa = \sqrt{4\hat{N} + 2}\sqrt{4\hat{N} + 6}BB \tag{B.4}$$

$$\hat{n} = 2\hat{N}, \tag{B.5}$$

Odd:

$$a^\dagger a^\dagger = \sqrt{4\hat{N} + 2}B^\dagger \tag{B.6}$$

$$aa = \sqrt{4\hat{N} + 6}B \tag{B.7}$$

$$a^\dagger a^\dagger a^\dagger a^\dagger = \sqrt{4\hat{N} + 2}\sqrt{4\hat{N} - 2}B^\dagger B^\dagger \tag{B.8}$$

$$aaaa = \sqrt{4\hat{N} + 6}\sqrt{4\hat{N} + 10}BB \tag{B.9}$$

$$\hat{n} = 2\hat{N} + 1. \tag{B.10}$$

We now use the techniques shown in section 2.3 to write $B^\dagger$ and B in terms of g and h:

$$B^\dagger = \sqrt{\overline{g}}h \tag{B.11}$$

$$B = h^\dagger\sqrt{\overline{g}}, \hat{N} = B^\dagger B = \overline{g} \tag{B.12}$$

where $\sqrt{\overline{g}} = -i\ln(g)/\theta$ (θ here, of course, refers to the θ found in the exchange relation of g and h). In terms of scalars then ($g = e^{i\alpha}$; $h = e^{i\beta}$; $\overline{g} = \frac{\alpha}{\theta}$, $A * B = Ae^{i\theta\overleftarrow{\partial_\beta}\overrightarrow{\partial_\alpha}}B$):

$$B^\dagger = \sqrt{\frac{\alpha}{\theta}} * e^{i\beta} = \sqrt{N} * e^{i\beta} = \sqrt{N}e^{i\beta} \tag{B.13}$$

$$B = e^{-i\beta} * \sqrt{\frac{\alpha}{\theta}} = \sqrt{N+1} * e^{-i\beta} = \sqrt{N+1}e^{-i\beta} \tag{B.14}$$

(in our case θ corresponds to $\hbar$).
In general

$$\begin{aligned} e^{ki\beta} * f(N) &= f(N-k) * e^{ki\beta} = f(N-k)e^{ki\beta} && \text{(B.15)} \\ e^{-ki\beta} &= f(N+k) * e^{-ki\beta} = f(N+k)e^{-ki\beta}. && \text{(B.16)} \end{aligned}$$

In terms of operators, our initial Hamiltonian would have the following form,

$$H(0,h,\hat{N}) = n_0(0,\hat{N}) + hn_1(0,\hat{N}) + n_1(0,\hat{N})h^\dagger + h^2 n_2(0,\hat{N}) + n_1(0,\hat{N})h^{\dagger^2}, \tag{B.17}$$

which translates too

$$\begin{aligned} H(0,\beta,N) &= n_0(0,N) + n_1(0,N-1)e^{i\beta} + n_1(0,N)e^{-i\beta} \\ &\quad + n_2(0,N-2)e^{2i\beta} + n_2(0,N)e^{-2i\beta}. \end{aligned} \tag{B.18}$$

We can use (2.21) and (B.18) to derive the flow equations. Firstly we see that

$$\begin{aligned} T_+(\ell) &= n_1(\ell,N-1)e^{i\beta} + n_2(\ell,N-2)e^{2i\beta} && \text{(B.19)} \\ T_-(\ell) &= n_1(\ell,N)e^{-i\beta} + n_2(\ell,N)e^{-2i\beta}. && \text{(B.20)} \\ & && \text{(B.21)} \end{aligned}$$

Since $\eta(\ell) = T_+(\ell) - T_-(\ell)$, our flow equation becomes

$$\frac{\partial H(\ell)}{\partial \ell} = [T_+, n_0]_* - [T_-, n_0]_* + 2[T_+, T_-]_*. \tag{B.22}$$

Next we work out the three Moyal brackets:

$$\begin{aligned}
[T_+, n_0]_* &= (n_0(N-1) - n_0(N))n_1(N-1)e^{i\beta} \\
&\quad +(n_0(N-2) - n_0(N))n_2(N-2)e^{2i\beta} && \text{(B.23)} \\
[T_-, n_0]_* &= (n_0(N+1) - n_0(N))n_1(N)e^{-i\beta} \\
&\quad +(n_0(N+2) - n_0(N))n_2(N)e^{-2i\beta} && \text{(B.24)} \\
[T_+, T_-]_* &= n_1(N-1)^2 - n_1(N)^2 + n_2(N-2)^2 - n_2(N)^2 + \\
&\quad +n_1(N-1)n_2(N-1)e^{-i\beta} - n_2(N)n_1(N+1)e^{-i\beta} \\
&\quad +n_1(N-2)n_2(N-2)e^{i\beta} - n_1(N)n_2(N-1)e^{i\beta}. && \text{(B.25)}
\end{aligned}$$

We can then obtain the flow equations by matching terms left and right with the same factor of $e^{ki\beta}$, where $k = -2, -1, 1, 2$. Doing this gives us

$$\begin{aligned}
\frac{\partial n_0}{\partial \ell} &= n_1(\ell, N-1)^2 - n_1(\ell, N)^2 + n_2(\ell, N-2)^2 - n_2(\ell, N)^2 && \text{(B.26)} \\
\frac{\partial n_1}{\partial \ell} &= n_1(\ell, N)(n_0(\ell, N) - n_0(\ell, N+1)) - 2n_1(\ell, N+1)n_2(\ell, N) \\
&\quad +2n_1(\ell, N-1)n_2(\ell, N-1) && \text{(B.27)} \\
\frac{\partial n_2}{\partial \ell} &= n_2(\ell, N)(n_0(\ell, N) - n_0(\ell, N+2)) && \text{(B.28)}
\end{aligned}$$

To find the initial conditions for n_0, n_1 and n_2, we will make use of (4.3) together with equations (B.1) to (B.10) and equations (B.13) to (B.16). After substitutions and being very careful with the Moyal product (we want to keep all the factors with β to the right, so that the Moyal products are exactly ordinary products), we arrive at the initial Hamiltonians for the even and odd sectors in term of N and β. To find $n_1(0, N)$, for example, we then match it to the function of N standing in front of $e^{-i\beta}$ (since the function infront of $e^{i\beta}$ would give us $n_1(0, N-1)$). After matching all the terms, we arrive at

Even:

$$n_0(0,N) = \hbar(4N+1) + \frac{\epsilon\hbar}{2}(4N+1) + \frac{\lambda\hbar^2}{4}(3+12N+24N^2) \quad \text{(B.29)}$$

$$n_1(0,N) = \left(\frac{\epsilon\hbar}{2} + \frac{\lambda\hbar^2}{4}(6+8N)\right)\sqrt{N+1}\sqrt{4N+2} \quad \text{(B.30)}$$

$$n_2(0,N) = \frac{\lambda\hbar^2}{4}\sqrt{N+1}\sqrt{N+2}\sqrt{4N+2}\sqrt{4N+6}, \quad \text{(B.31)}$$

Odd:

$$n_0(0,N) = \hbar(4N+3) + \frac{\epsilon\hbar}{2}(4N+3) + \frac{\lambda\hbar^2}{4}(15+36N+24N^2) \quad \text{(B.32)}$$

$$n_1(0,N) = \left(\frac{\epsilon\hbar}{2} + \frac{\lambda\hbar^2}{4}(10+8N)\right)\sqrt{N+1}\sqrt{4N+6} \quad \text{(B.33)}$$

$$n_2(0,N) = \frac{\lambda\hbar^2}{4}\sqrt{N+1}\sqrt{N+2}\sqrt{4N+6}\sqrt{4N+10}, \quad \text{(B.34)}$$

where we have re-inserted the factors of $\hbar$, since we shall be using them in a short while.

If we make the association $N = \frac{q}{\hbar}$, then we may write (B.26) to (B.28) as

$$\frac{\partial n_0}{\partial \ell} = n_1(\ell, q-\hbar)^2 - n_1(\ell,q)^2 + n_2(\ell, q-2\hbar)^2 - n_2(\ell,q)^2 \quad \text{(B.35)}$$

$$\frac{\partial n_1}{\partial \ell} = n_1(\ell,q)(n_0(\ell,q) - n_0(\ell,q+\hbar)) - 2n_1(\ell,q+\hbar)n_2(\ell,q) + 2n_1(\ell,q-\hbar)n_2(\ell,q-\hbar) \quad \text{(B.36)}$$

$$\frac{\partial n_2}{\partial \ell} = n_2(\ell,q)(n_0(\ell,q) - n_0(\ell,q+2\hbar)). \quad \text{(B.37)}$$

To first order in $\hbar$, these become

$$\frac{\partial n_0}{\partial \ell} = -2\hbar\left(\frac{\partial n_1^2}{\partial q} + 2\frac{\partial n_2^2}{\partial q}\right) \quad \text{(B.38)}$$

$$\frac{\partial n_1}{\partial \ell} = -\hbar\left(4n_2(\ell,q)\frac{\partial n_1}{\partial q} + n_1(\ell,q)\left[\frac{\partial n_0}{\partial q} + 2\frac{\partial n_2}{\partial q}\right]\right) \quad \text{(B.39)}$$

$$\frac{\partial n_2}{\partial \ell} = -2\hbar\, n_2(\ell,q)\frac{\partial n_0}{\partial q}. \quad \text{(B.40)}$$

These agree with (4.45), (4.46) and (4.47) except for certain factors of two. This comes from the fact that we are essentially combining the parts that belong to $e^{i\beta}$ and $e^{-i\beta}$ into a $\cos(\theta)$ in equations (4.45) to (4.47), which is only possible to lowest order.

BIBLIOGRAPHY

[1] Wegner F 1994 *Annalen der Physik* **506(2)** 77.

[2] Glazek S D and Wilson K G 1994 *Phys. Rev.* D **49** 4214

[3] Moyal J E 1949 *Quantum Mechanics as a Statistical Theory*, Proc. Camb. Phil. Soc. 45 99.

[4] Griffiths D J 1994 *Introduction to Quantum Mechanics* (Prentice Hall, Inc., Englewood Cliffs, New Jersey).

[5] Schwabl F 1992 *Quantum Mechanics* (Springer-Verlag, Berlin).

[6] Brack M and Bhaduri R K 1997 *Semiclassical Physics* (Addison-Wesley Publishing Company, Inc., Reading, Massachusetts).

[7] Gradshteyn I S and Ryzhik I M 1965 *Table of Integrals, Series, and Products* (Academic Press, New York and London).

[8] Bartlett B 2003 *Flow Equations for Hamiltonians from Continuous Unitary Transformations* (MSc. Thesis, University of Stellenbosch).

[9] Kriel J N, Morozov A Y and Scholtz F G 2004 *J. Phys. A: Math. Gen.* **37** 305.

[10] Brockett R W 1991 *Linear Algebra and its Applications* **146** 79

[11] Scholtz F G, Bartlett B H and Geyer H B 2003 *Phys. Rev. Lett* **91** 080602.

[12] Knetter C 2003 *Perturbative Continuous Unitary Transformations: Spectral Properties of Low Dimensional Spin Systems* (Ph.D Thesis, Köln University).

[13] Knetter C, Schmidt K P and Uhrig G S 2003 *J. Phys. A: Math. Gen.* **36** 7889.

[14] Scholtz F G and Geyer H B 2006 *Phys. Lett. B* **634** 84.

[15] Kriel J N 2005 *Non-perturbative Flow Equations from Continuous Unitary Transformations* (MSc. Thesis, University of Stellenbosch).

[16] Gardiner C W 1991 *Quantum Noise* (Springer-Verlag, Berlin).

[17] Antonsen F 1998 *Int. J. Theor. Phys.* **37** 697.

[18] Garg A 2000 *Am. J. Phys.* **68** 430.

[19] Robnik M, Salasnich L and Vraničar M 2000 *Prog. Theor. Phys. Suppl.* **139** 550.